chemosensors

MDPI

Review

Chemosensors for H_2O_2 Detection: Principles, Active Materials, and Applications

Meng Zhou [1,2], Hui Sun [3], Shuai Chen [1,2,*], Mingna Yang [2], Rongqing Dong [2], Xiaomei Yang [4] and Ling Zang [4,*]

[1] School of Pharmacy, Jiangxi Science & Technology Normal University, Nanchang 330013, China; zhoumeng1512022@163.com
[2] Jiangxi Provincial Key Laboratory of Flexible Electronics, Nanchang 330013, China; yangmingna1023@163.com (M.Y.); drongqing@163.com (R.D.)
[3] Binzhou Testing Center, Binzhou 256600, China; shlbl1990@126.com
[4] Department of Materials Science and Engineering, Nano Institute of Utah, University of Utah, Salt Lake City, UT 84112, USA; jaimee@eng.utah.edu
* Correspondence: shuaichen@jxstnu.edu.cn (S.C.); lzang@eng.utah.edu (L.Z.); Tel.: +1-801-587-1551 (L.Z.); Fax: +1-801-581-4816 (L.Z.)

Abstract: Hydrogen peroxide (H_2O_2), a common oxidant present in the environment, food, and biological systems, has wide-ranging applications. While H_2O_2 is generally considered non-toxic, prolonged or repeated exposure to high concentrations can be harmful, making its accurate detection crucial in environmental monitoring, food safety, healthcare, and other fields. This review delves into the recent advancements in H_2O_2 detection methods, with a particular focus on chemosensors. We comprehensively summarize the fundamental principles of various chemosensor principles (e.g., colorimetric, fluorescence, chemiluminescence, electrochemical, and chemiresistive approaches), active materials, and diverse applications. Additionally, we discuss the current challenges and future prospects in this field, emphasizing the need for innovative materials and advanced sensing technologies to meet the growing demand for highly sensitive, accurate, reliable, real-time, and cost-effective H_2O_2 detection solutions.

Keywords: chemosensor; H_2O_2 detection; optical; electrochemical; chemiresistive

Received: 10 December 2024
Revised: 27 January 2025
Accepted: 3 February 2025
Published: 6 February 2025

Citation: Zhou, M.; Sun, H.; Chen, S.; Yang, M.; Dong, R.; Yang, X.; Zang, L. Chemosensors for H_2O_2 Detection: Principles, Active Materials, and Applications. *Chemosensors* **2025**, *13*, 54. https://doi.org/10.3390/chemosensors13020054

1. Introduction

Hydrogen peroxide (H_2O_2) is a vital chemical and biomarker widely utilized across various fields, including industrial processes, environmental disinfection, pharmaceutical reactions, food analysis, and clinical diagnostics [1–3]. Its versatile characteristics, functioning as an oxidant, reducing agent, or catalyst, make it an essential component in numerous chemical and biological processes. Additionally, its moderate oxidizing properties enable widespread use as a bleaching agent, preservative, germicide, and disinfectant on an industrial scale [4–7]. However, the strong oxidizing capacity of H_2O_2 can lead to adverse effects on human integument, ocular structures, and respiratory tracts, as well as the activities of other organisms, when present in the environment at concentrations exceeding recommended limits [8,9]. Furthermore, an imbalance in H_2O_2 levels may compromise the quality, safety, and efficacy of products such as pharmaceuticals [10].

Accurate detection of H_2O_2 in both gaseous and liquid phases is, therefore, of critical importance [11,12]. However, achieving reliable detection results presents several challenges:

(1) High Reactivity: H_2O_2 is colorless, odorless, and volatile, making it prone to decomposition, particularly under light, heat, or in the presence of catalysts like metal ions. This instability complicates accurate detection, as decomposition products (H_2O and O_2) often interfere with measurements. Additionally, the strong oxidizing nature of H_2O_2 may lead to undesired reactions with other substances during detection.
(2) Limited Selectivity: The presence of other oxidative chemicals (e.g., O_2, O_3) in real-world samples can interfere with H_2O_2 detection, leading to false positives or negatives by producing similar signals or reacting with detection reagents.
(3) Environmental Sensitivity: H_2O_2 coexists with H_2O, a challenge for gas sensors. Its volatility and sensitivity to environmental conditions, such as temperature and light, demand strict control during testing to ensure accuracy.
(4) Sample Preparation: Preventing H_2O_2 decomposition, removing interferences, and enriching analyte concentrations require labor-intensive preparation, making detection methods prone to noise or susceptible to missed low concentrations.
(5) Instrumental Limitations: Analytical instruments may face constraints in detection range, precision, and reproducibility, affecting result reliability.
(6) Cost and Accessibility: Traditional methods, such as chemical titration, are time-consuming, require skilled operators, and are often restricted to research settings. Advanced methods may demand expensive equipment, reagents, and expertise, limiting accessibility.

Despite these challenges, a variety of analytical techniques have been developed for H_2O_2 detection, each with unique principles and applications. For instance, ion chromatography provides low detection limits, wide ranges, and resistance to interference, making it ideal for water samples with coexisting substances [13]. High-performance liquid chromatography offers high separation efficiency and sensitivity, suitable for complex samples like wastewater, food, and pharmaceuticals [14–17]. Raman spectroscopy, being non-destructive and requiring no sample pretreatment, is well-suited for detecting H_2O_2 in solids, liquids, and gases [10]. Compared to these methods, chemosensors, particularly electrochemical sensors [18,19], stand out for their fast response, simplicity, cost-effectiveness, and real-time monitoring capabilities [20]. Techniques like colorimetry [21], fluorescence [22], and chemiluminescence [23] also provide high sensitivity and selectivity by leveraging specific chemical reaction mechanisms [24].

The choice of detection method depends on application requirements and conditions to ensure accuracy and reliability. Recent advances in material science, nanotechnology, and biotechnology have driven the development of novel materials and architectures for improved sensing performance [25–28]. However, in order to effectively analyze the results of chemical sensors and assess their reliability in practical applications, it is particularly important to understand the permissible limits of H_2O_2 in different environments and various applications. These permissible limits not only provide a benchmark for evaluating sensor performance but also help ensure the accuracy and practicality of the detection results. While previous reviews have focused on fluorescent probes and metal-based materials for H_2O_2 detection, chemosensors have received comparatively less attention [29–31]. This review aims to comprehensively summarize the latest advancements in chemosensors for H_2O_2 detection, focusing on detection mechanisms, materials, and applications (Figure 1).

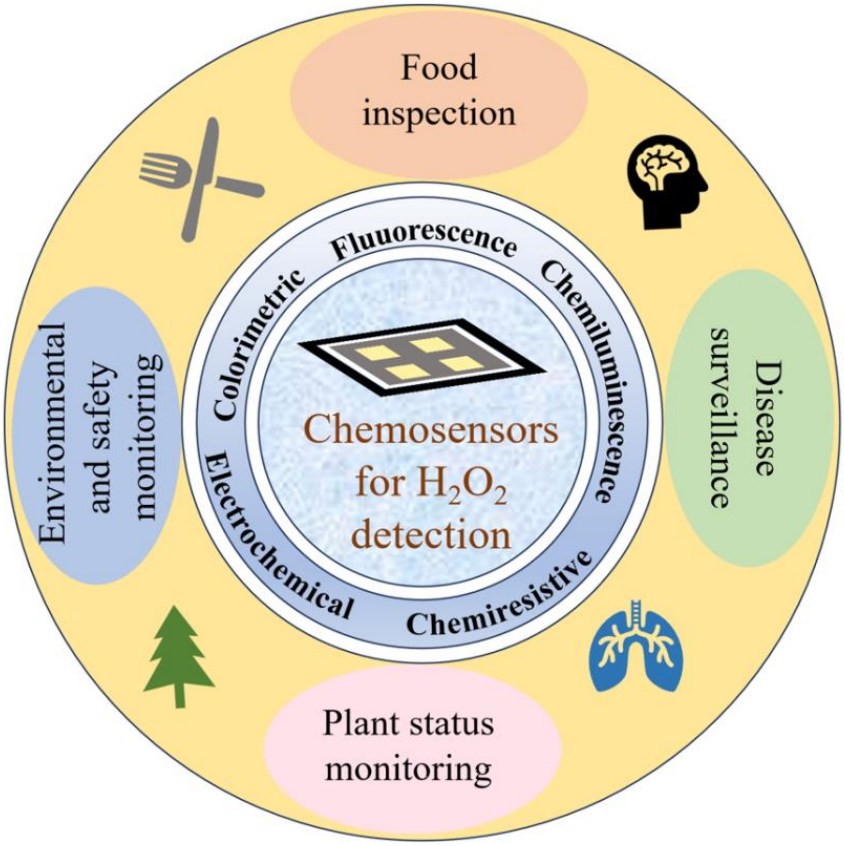

Figure 1. Schematic illustration of the response mechanisms and primary applications of chemosensors for H_2O_2 detection.

2. Mechanisms of Chemosensors for H_2O_2 Detection

The methods for detecting H_2O_2 are diverse and tailored to various applications. Among chemical titration techniques, potassium permanganate titration is widely used, relying on the redox reaction between potassium permanganate and H_2O_2 to determine its concentration based on the amount of potassium permanganate consumed [1]. While this method is straightforward and easy to perform, its accuracy may be affected by human error. Biosensor-based methods leverage the specific interactions of biomolecules, offering strong specificity and high sensitivity. These methods are extensively employed in biomedical research and food testing [25,32]. Raman spectroscopy, on the other hand, provides non-contact and non-destructive testing, making it valuable for applications such as cultural heritage preservation. However, this technique comes with high instrument costs and relatively low sensitivity [10]. Chemosensors for H_2O_2 detection primarily rely on five key strategies based on optical and electrical principles. Optical sensors detect H_2O_2 by monitoring changes in spectrophotometric absorbance (colorimetric), emission intensity (fluorescence), or radiation intensity (chemiluminescence) induced by its presence [21–23]. In contrast, electrical sensors measure H_2O_2 concentrations indirectly by detecting electrical signals—such as current or voltage (electrochemical approaches) and resistance (chemiresistive approaches)—generated by the oxidation or reduction in H_2O_2 on the sensor electrode [18,19]. Table 1 summarizes a range of chemical sensors for H_2O_2 detection, highlighting diverse detection mechanisms, including colorimetric, fluorescent, chemiluminescent, electrochemical, and chemiresistive methods. These sensors differ in their applicability to various physical states, lowest detection limits (LDL), and linear ranges, offering versatile options for H_2O_2 detection across multiple fields.

Table 1. Comparison of diverse chemosensors for H_2O_2 detection.

Mechanism	Sensor Materials	LDL	H_2O_2 (Physical State)	Linear Range	Ref.
Colorimetric	Fe_3O_4-Fe^0/Fe_3C	67.1 pM	liquid	0.01–0.25 μM	[33]
Colorimetric	XH-2	0.091 μM	liquid	0–120 μM	[34]
Colorimetric	AgNPs@MOF	0.17 μM	liquid	0.5–50 μM	[35]
Colorimetric	RuO_2 NPs	0.39 μM	liquid	1–10,000 μM	[36]
Colorimetric	HRP/$Cu_3(PO_4)_2{\cdot}3H_2O$	0.5 μM	liquid	5–500 μM	[37]
Colorimetric	$CoCO_3$/TMB	1.39 μM	liquid	5.0–75.0 μM	[38]
Colorimetric	$NiFe_2O_4$/CNTs	2.2 μM	liquid	5–60 μM	[39]
Colorimetric	Zr/MOF/PVP	2.76 μM	liquid	10–800 μM	[40]
Colorimetric	Ag@CMs	5 μM	liquid	5–200 μM	[41]
Colorimetric	MOF-818	9.02 μM	liquid	13.3–10,000 μM	[42]
Colorimetric	Gox/TMB	30 μM	liquid	500–6000 μM	[43]
Colorimetric	Ti (IV) oxo complexes	0.1 ppm	gaseous	0–1.0 ppm	[44]
Colorimetric	AgNPs	0.216 ppm	gaseous	0–300 ppm	[45]
Colorimetric	Paper/KI	0.015 meq/Kg	liquid	0.01–30 meq/Kg	[46]
Colorimetric	BPCN NSs	1.0 μM	liquid	0–1000 μM	[47]
Fluorescent	Fe_3Ni-MOF-NH_2	0.005 μM	liquid	0.01–16 μM	[48]
Fluorescent	LBM	0.013 μM	Liquid	0–50 μM	[49]
Fluorescent Electrochemical	TAPP	0.03 μM 0.3 μM	liquid	0.105–0.39 μM 1–50 μM	[50]
Fluorescent	chalcones, primary amines, and β-ketoesters	1.08 μM	liquid	0–50 μM	[51]
Fluorescent	$(dfppy)_2$Ir-bpy-NH_2	3.084 μM	liquid	0–500 μM	[52]
Fluorescent	ARS/GAL	7.4 μM	liquid	60–500 μM	[53]
Fluorescent	TATP	0.2 ppm	gaseous	-	[54]
Chemiluminescent	Hemoglobin/luminol	308 μM	liquid	500–12,000 μM	[55]
Electrochemical	FET/Cyt c	100 fM	liquid	1×10^2–1×10^{14} fM	[56]
Electrochemical	pillar[3]arene[2] quinone/ferrocene	0.0003 μM	liquid	0.001–100 μM	[57]
Electrochemical	Fe_3O_4@MoS_2-AuNPs	0.08 μM	liquid	1–120 μM	[58]
Electrochemical	PtNPs/MWCNTs	0.2 μM	liquid	0.5–100 μM	[59]
Electrochemical	AuNPs/CeO_2	0.21 μM	liquid	0.01–100,000 μM	[60]
Electrochemical	SWCNTs/MnO_2	0.31 μM	liquid	2–5000 μM	[61]
Electrochemical	Te NSs	0.47 μM	liquid	0.2–5 μM	[62]
Electrochemical	TiO_2 NTs	0.98 μM	liquid	3–200 μM	[63]
Electrochemical	Ta/Pt/Ti	1 μM 42 ppb	Liquid gaseous	-	[64]
Electrochemical	BGN/GNA	1.183 μM	liquid	10–100,000 μM	[65]
Electrochemical	CuO Co_3O_4	1.34 μM 1.05 μM	liquid liquid	20–7000 μM	[66]
Electrochemical	CuNPs/ITO	1.73 μM	liquid	1–500 μM	[67]
Electrochemical	PtNP/rGO–CNT/PtNP/SPCE	4.3 μM	liquid	25–1000 μM	[68]
Electrochemical	LSG	4.6 μM	liquid	20–3400 μM	[69]
Electrochemical	AuNPs/SnO_2NFs	6.67 μM	liquid	49.98–3937.21 μM	[70]
Electrochemical	Cu-exchanged zeolitic volcanic tuff	10 μM	liquid	10–30,000 μM	[71]
Electrochemical	ZnO/laser-induced graphene	190 μM	liquid	800–14,600 μM	[72]
Chemiresistive	PEDOT:PSS/PEDOT	1.0 ppm	gaseous	0–10.5 ppm	[73]
Chemiresistive	PEDOT:PSS-ATO/PEDOT	1.0 ppm	gaseous	1.0–10.5 ppm	[74]

2.1. Optical Chemosensors

Optical detection technology has emerged as a particularly active area of interest in H_2O_2 sensing [75]. Compared to complex analytical techniques such as chromatography or mass spectrometry, which require sophisticated instrumentation and extensive training, spectrophotometric methods offer unique advantages. While potentially less sensitive, they are valued for their non-contact operation, cost-effectiveness, simplicity, and suitability for real-time monitoring [76]. This approach typically involves a chemical reaction between H_2O_2 and an optical probe or sensing compound. The concentration of H_2O_2 is indirectly determined by monitoring changes in optical signals, such as color shifts or fluctuations in fluorescence intensity, caused by the reaction. However, these methods can face specificity challenges due to interference from other compounds with similar redox properties in the sample. A significant challenge lies in the design and synthesis of spectrophotometrically active probe molecules that enhance sensitivity, specificity, and stability, underscoring the need for continued innovation in this field.

2.1.1. Colorimetric Sensor

Colorimetric sensors rely on color changes resulting from the interaction between H_2O_2 and specific probing compounds [22]. These mechanisms typically involve chemical reactions or physical interactions with colorimetric probes such as chemical indicators, dyes, or nanomaterials [77]. The color change can be observed directly with the naked eye or measured using spectroscopic instruments, enabling both qualitative and quantitative detection of H_2O_2.

For example, Zhang et al. [41] utilized Ag nanoparticles (Ag NPs) modified cellulose membranes (Ag@CMs) for the simultaneous colorimetric detection of mercury ions (Hg^{2+}) and H_2O_2 through in-situ reactions (Figure 2a). The Ag@CMs demonstrated a visual LDL for H_2O_2 of 5 μM and an effective detection range of 5–200 μM. In another approach, Zhang et al. [43] developed a cost-effective, portable paper-based colorimetric sensor for the rapid detection of H_2O_2 and related biomarkers in fruits such as apples, pears, and coconuts. This sensor employed the selective reaction of glucose oxidase (GOx) with H_2O_2 as a sensitive material (Figure 2b). It exhibited a linear response and high sensitivity within the concentration range of 500–6000 μM (Figure 2c).

However, liquid-phase methods for H_2O_2 vapor detection are hindered by interference from humidity and other gases, necessitating more efficient approaches. To address this, Zang et al. [44] developed a colorimetric sensor for H_2O_2 vapor (Figure 2d) using a cellulose fiber network derived from ordinary paper towels combined with a Ti(IV) oxide composite. This system reacted with H_2O_2 to produce a color change from colorless to yellow, with a linear range of 0–1.0 ppm and an LDL of 0.1 ppm.

Metal-organic frameworks (MOFs) have also shown promise as emerging peroxidase-mimetic enzymes with significant application potential [78]. For instance, Wang et al. [40] synthesized Zr-MOF-PVP nanocomposites using a solvothermal method and polyvinylpyrrolidone (PVP) as a surfactant. These nanocomposites demonstrated peroxidase-like activity, reacting with H_2O_2 and the chromogenic substrate 3,3′,5,5′-tetramethylbenzidine (TMB) to produce a color change from transparent to pink. This method provided a linear detection range of 10–800 μM and an LDL of 2.76 μM. Similarly, Wu et al. [39] synthesized $NiFe_2O_4$/carbon nanotube (CNT) composites using atomic layer deposition technology, which exhibited peroxidase-like properties for gas-phase sensing. These sensors achieved high sensitivity, detecting H_2O_2 concentrations as low as 2.2 μM, and were applied to glucose detection in juice samples.

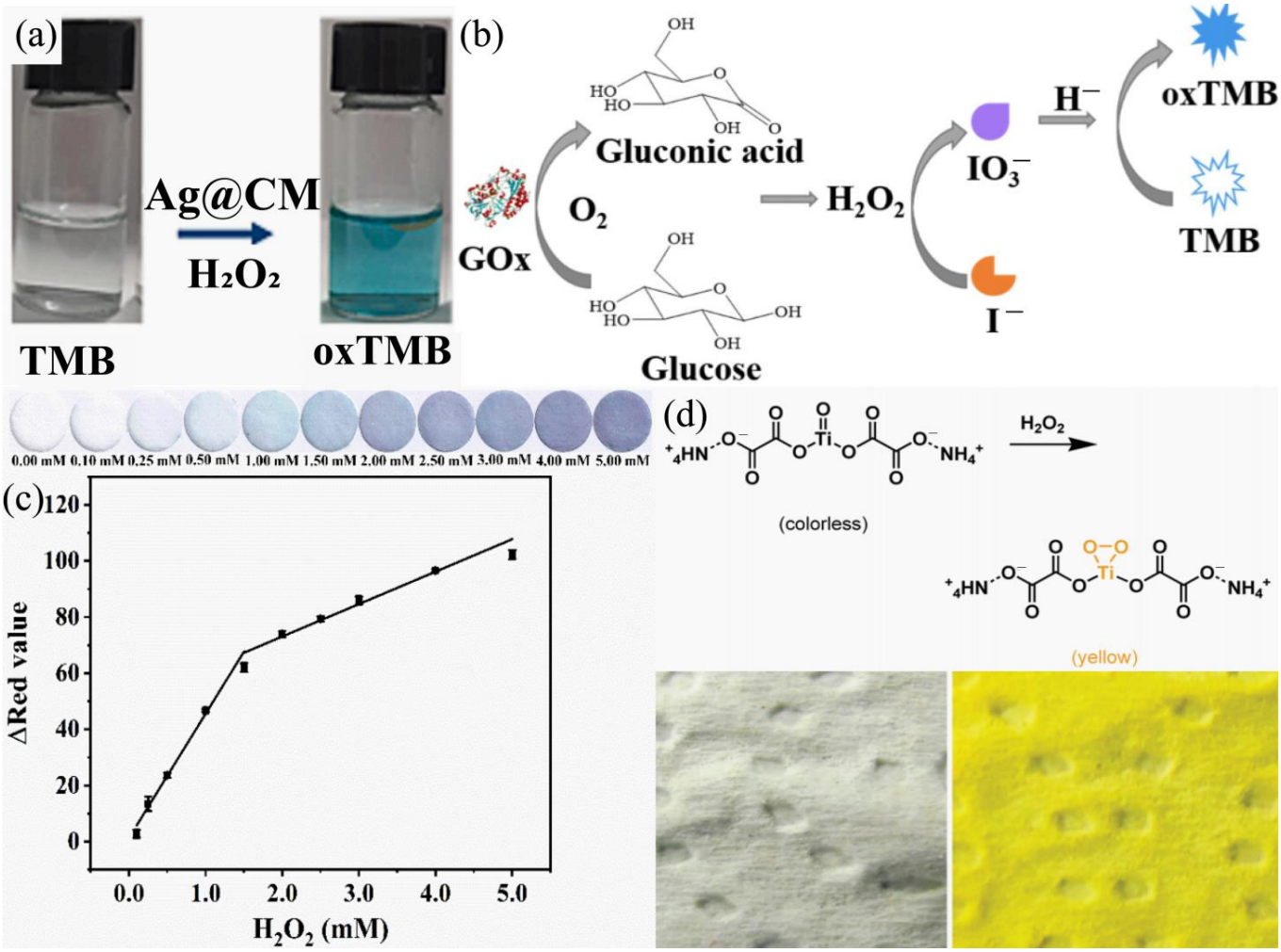

Figure 2. (**a**) The colorimetric mechanism of Ag@CMs towards H_2O_2 solution [41]; (**b**) Mechanism of paper-based colorimetric H_2O_2 sensor relying on KI-TMB; (**c**) Calibration curves of the paper-based colorimetric sensor relying on KI-TMB in different concentration ranges of H_2O_2 [43]; (**d**) The colorimetric mechanism of Ti (IV) oxide complex sensor for H_2O_2 vapor detection [44].

In summary, colorimetric sensing of H_2O_2 in solutions or vapors enables visual observation of color changes without requiring complex instruments, making it suitable for rapid and on-site detection. These methods are simple to operate and generally do not require extensive sample preparation. However, while they can qualitatively detect H_2O_2, accurate quantitative analysis often requires calibration with instrumental techniques.

2.1.2. Fluorescent Sensor

Fluorescent detection is one of the most prevalent and effective spectrophotometric methods for H_2O_2 sensing [79]. Ingeniously designed probe molecules enable significant changes in fluorescence signals, either through enhancement or quenching, upon reaction with H_2O_2. These changes facilitate highly sensitive qualitative and quantitative detection [80]. Typically, phenolic fluorophore-based probes release fluorophores through oxidation by H_2O_2, resulting in notable fluorescence intensity changes depending on their chemical structures [81].

As a byproduct of cellular aerobic metabolism, excessive H_2O_2 production can lead to diseases such as Parkinson's and Alzheimer's [82]. Fluorescent sensors are especially valuable for detecting trace levels of H_2O_2, making them indispensable in studying their roles in biological systems [83]. Most research in this area focuses on the design and syn-

thesis of novel fluorophore molecules. For instance, Wu et al. [48] developed a fluorescent sensor based on nano-MOFs (Fe), achieving highly sensitive H_2O_2 detection with detection limits in the nanomolar range. The sensor's response was attributed to the catalytic properties of MOF-Fe and the oxidation of TMB, with fluorescence intensity increasing as H_2O_2 concentration rose. González-Ruiz et al. [51] synthesized dihydro-m-terphenyl derivatives as fluorescent chemodosimeters for H_2O_2 detection, exhibiting a "turn-on" fluorescence signal (Figure 3a). The compounds, initially non-fluorescent, underwent oxidative dehydrogenation in the presence of H_2O_2, forming aromatic derivatives and a delocalized conjugated system, which generated fluorescence. This sensor achieved a detection limit of 1.08 μM and demonstrated a linear response in the 0–50 μM range.

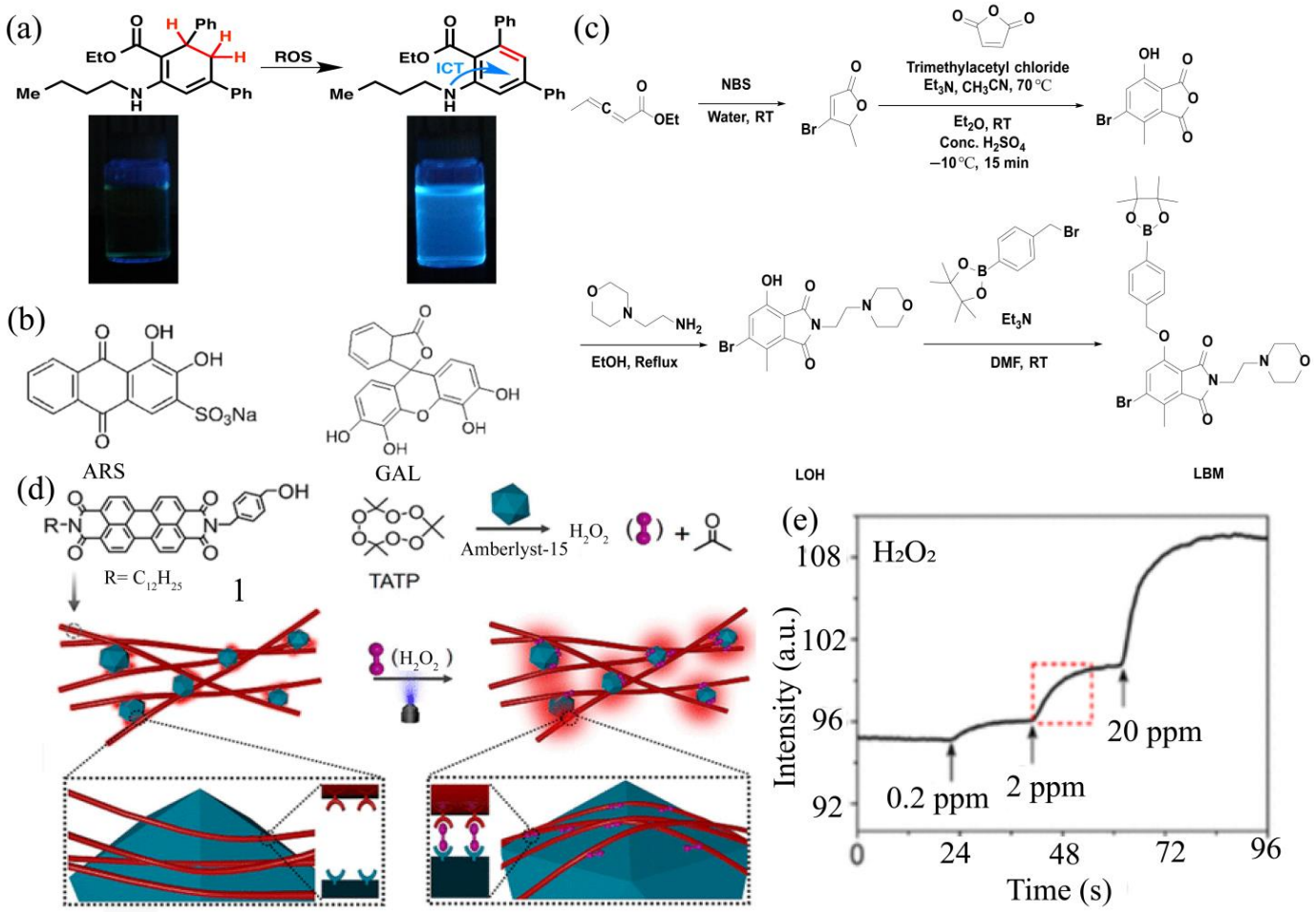

Figure 3. (**a**) Sensing mechanism of fluorescent dihydro-*m*-terphenyl derivative sensor towards H_2O_2 solution [51]; chemical structure of (**b**) ARS, GAL [53]; (**c**) LBM [49]; (**d**) schematic of the fluorescence enhancement mechanism of TATP sensor; and (**e**) its response in different concentration ranges of H_2O_2 solution [54].

Li et al. [53] created fluorescent sensors (ARS-CBA and GAL-CBA) via the self-assembly of aromatic boronic acid with ARS and GAL to detect H_2O_2 in biological samples (Figure 3b). While GAL itself contains multiple -OH groups, fluorescence enhancement occurred only when ARS was bound with boronic acid. The ARS-CBA sensor had a detection limit of 7.4 μM and a rapid response time of 5 min, whereas GAL-CBA showed prolonged response times. An et al. [49] synthesized a fluorescent probe (LBM) combining an H_2O_2-reactive arylboronic acid group and a mycophenolic acid recognition unit (Figure 3c). The probe achieved a detection limit of 0.013 μM and a linear range of 0–50 μM, with significant fluorescence intensity enhancements for intracellular H_2O_2 detection. These probes demon-

strated specific recognition of H_2O_2 in liquid systems without interfering with normal physiological functions. However, photobleaching under prolonged illumination remains a challenge, potentially compromising detection accuracy and stability.

In addition to liquid-phase detection for environmental, food, and biological analysis, gaseous H_2O_2 monitoring is critical for safety and health. Yu et al. [54] developed a hybrid fluorescent sensor system combining fluorescent nanofibers and amberlyst-15 particles for triacetone triperoxide (TATP) detection (Figure 3d). Robust hydrogen bonding between the nanofibers and amberlyst-15 enhanced photoluminescence. Upon exposure to H_2O_2 vapor, the hydrogen bond interaction was regulated, resulting in rapid fluorescence enhancement. The system exhibited significant fluorescence intensity changes for H_2O_2 concentrations up to 2 ppm and the response can be achieved within 5 s (Figure 3e), maintaining high sensitivity even in the presence of interferences like acetone and ethanol. Fluorescent sensors continue to demonstrate great potential for both liquid and vapor-phase H_2O_2 detection, with advancements in probe design driving improved sensitivity, specificity, and application scope.

2.1.3. Chemiluminescent Sensor

Unlike color changes in absorption spectra or fluorescence on/off mechanisms, chemiluminescence detection relies on measuring luminescence intensity generated by H_2O_2 participating in specific chemical reactions [52,84]. This method is widely used in constructing biosensors for various applications, including environmental monitoring, biomedical analysis, food safety, and more [10]. Chemiluminescence is commonly employed in the form of chemiluminescent immunoassays, which combine the high specificity of immune responses with the high sensitivity of chemiluminescence detection technology [85].

For instance, Teniou et al. [55] developed a chemiluminescence probe using hemoglobin (Hb) as a biological receptor. The heme group in Hb, acting as an electroactive center, catalyzed the reaction of H_2O_2 with luminescent agents (e.g., luminol), producing light (Figure 4a). The chemiluminescence signal decreased with increasing H_2O_2 concentration, indicating a strong correlation between the two (Figure 4b). This method demonstrated high sensitivity, with an LDL of 0.308 mM, and good repeatability, ensuring test accuracy. Chemiluminescence sensors offer several advantages, including high sensitivity, minimal background interference (as there is no background light signal), and straightforward operation, making them suitable for on-site and real-time monitoring. Furthermore, this approach avoids the complex design requirements of fluorescence probes. However, the detection system may be affected by external factors such as light or temperature fluctuations, requiring appropriate corrective measures for accurate results. Additionally, the method often requires specialized equipment.

Yoon et al. [86] explored chemosensing detection of H_2O_2/reactive oxygen species (ROS) using dual-modal probes 2a–c (Figure 4c) by comparing photoluminescence (PL) and electrochemiluminescence (ECL) methods. When excited at 500 nm, probes 2a (Figure 4d) and 2b (Figure 4e) exhibited strong emission at 520 nm, with their fluorescence peaks shifting to 500 nm as H_2O_2 concentrations increased. Meanwhile, probe 2c displayed fixed fluorescence at 490 nm with intensity strengthening (Figure 4f). The PL method exhibited higher selectivity, while the ECL method achieved greater sensitivity, with an LDL of 2.698 μM. Combining these two mechanisms improved the ability to distinguish between diabetic and normal models through principal component analysis, showcasing the potential of these dual-modal probes for diabetes diagnosis. Notably, ECL is a chemiluminescence phenomenon occurring during electrochemical reactions at an electrode in a solution containing H_2O_2 and an inorganic metal (e.g., Ir) complex as the luminophore. This combination of photoluminescence and electrochemiluminescence highlights the versatility of chemiluminescent sensors for diverse applications.

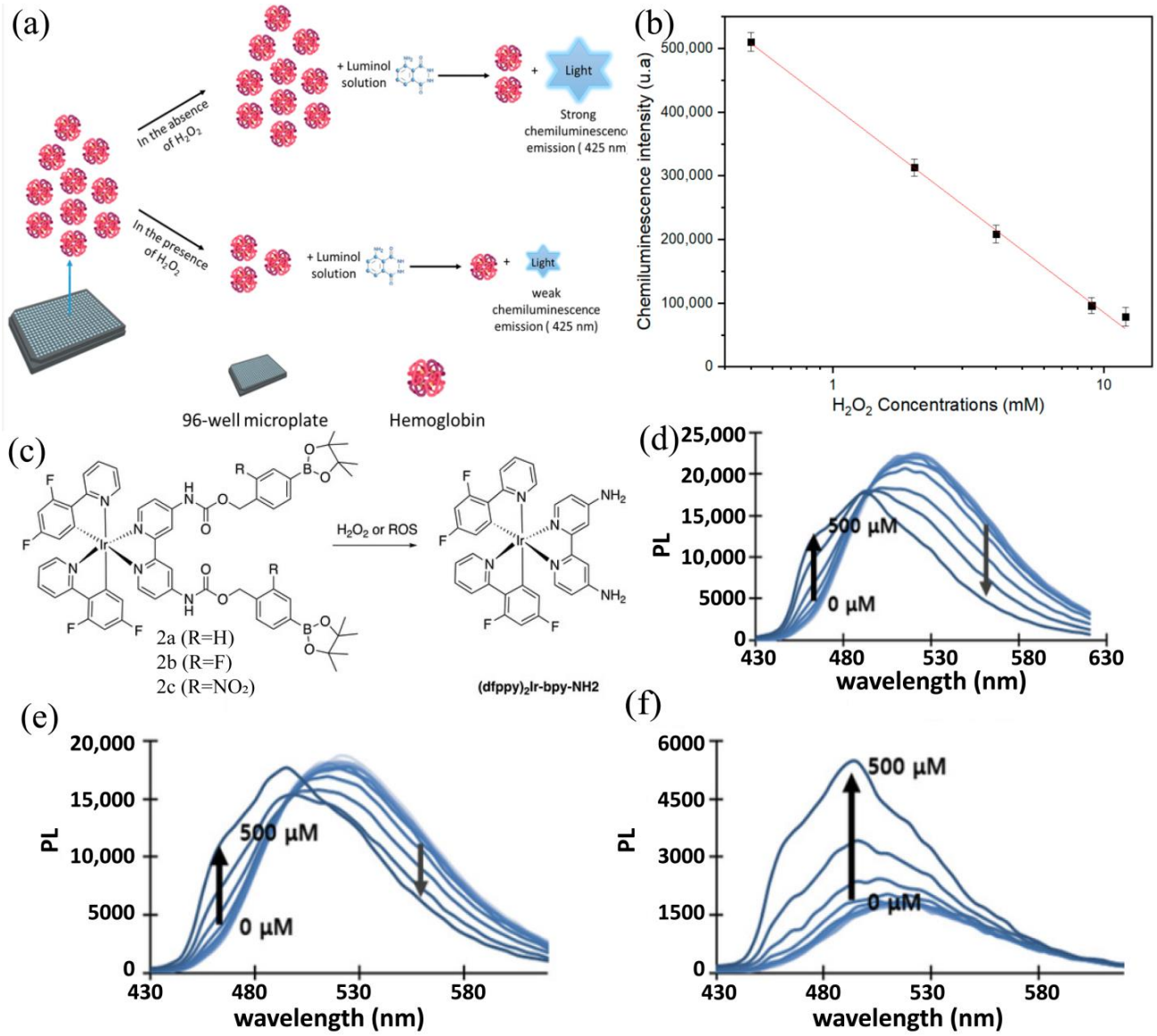

Figure 4. The sensing mechanism Hb based chemiluminescence method (**a**), and (**b**) the calibration curve obtained for an H_2O_2 solution in the concentration range of 0.5–12 mM [55]. (**c**) Molecular structures of the PL and ECL probes (2a–2c) and their sensing reaction, as well as the PL spectra changes (**d**–**f**) observed for H_2O_2 solution in the concentration range of 0–500 μM [86].

2.2. Electrical Chemosensors

2.2.1. Electrochemical Sensor

Compared to optical signals, electrical signals, especially electrochemical and chemiresistive modes, are easier to manipulate and integrate into practical applications, making them ideal for chemosensor construction [18]. Electrochemical sensors are often more cost-effective than spectrophotometric or chemiluminescent methods, both in terms of equipment and operational costs [87,88]. Additionally, their ease of integration into automated systems reduces the need for skilled operators and extensive sample preparation. These attributes make electrochemical methods highly suited for real-time and on-site monitoring of H_2O_2 in environmental pollutant treatment, industrial process control, and other fields.

Electrochemical detection of H_2O_2 typically relies on redox reactions occurring at the electrode surface, with signal changes in current or potential used to quantify concentrations [89,90]. Most sensors employ a three-electrode system (working electrode, counter electrode, and reference electrode) in an electrolyte environment. However, this configu-

ration may be affected by electrode conditions and the presence of other electrochemical species in the sample or environment.

Various electrochemical methods, including enzymatic reactions, amperometry, and cyclic voltammetry (CV), have been employed for H_2O_2 detection. The construction of high-efficiency working electrodes remains a core area of research. For instance, Zanoni et al. [72] combined ZnO with laser-induced graphene, comparing photoluminescence (PL) and CV methods for H_2O_2 detection. Their approach achieved low LDLs of 800–14,600 µM. Zakaria et al. [61] used CV to fabricate nanostructured composites of single-walled carbon nanotubes (SWCNTs) and MnO_2, modifying glassy carbon electrodes (GCE) (Figure 5a). These sensors showed high sensitivity (linear range: 2–5000 µM) and stability at physiological pH (7.4), with a correlation coefficient of 0.9822, demonstrating high reliability (Figure 5b).

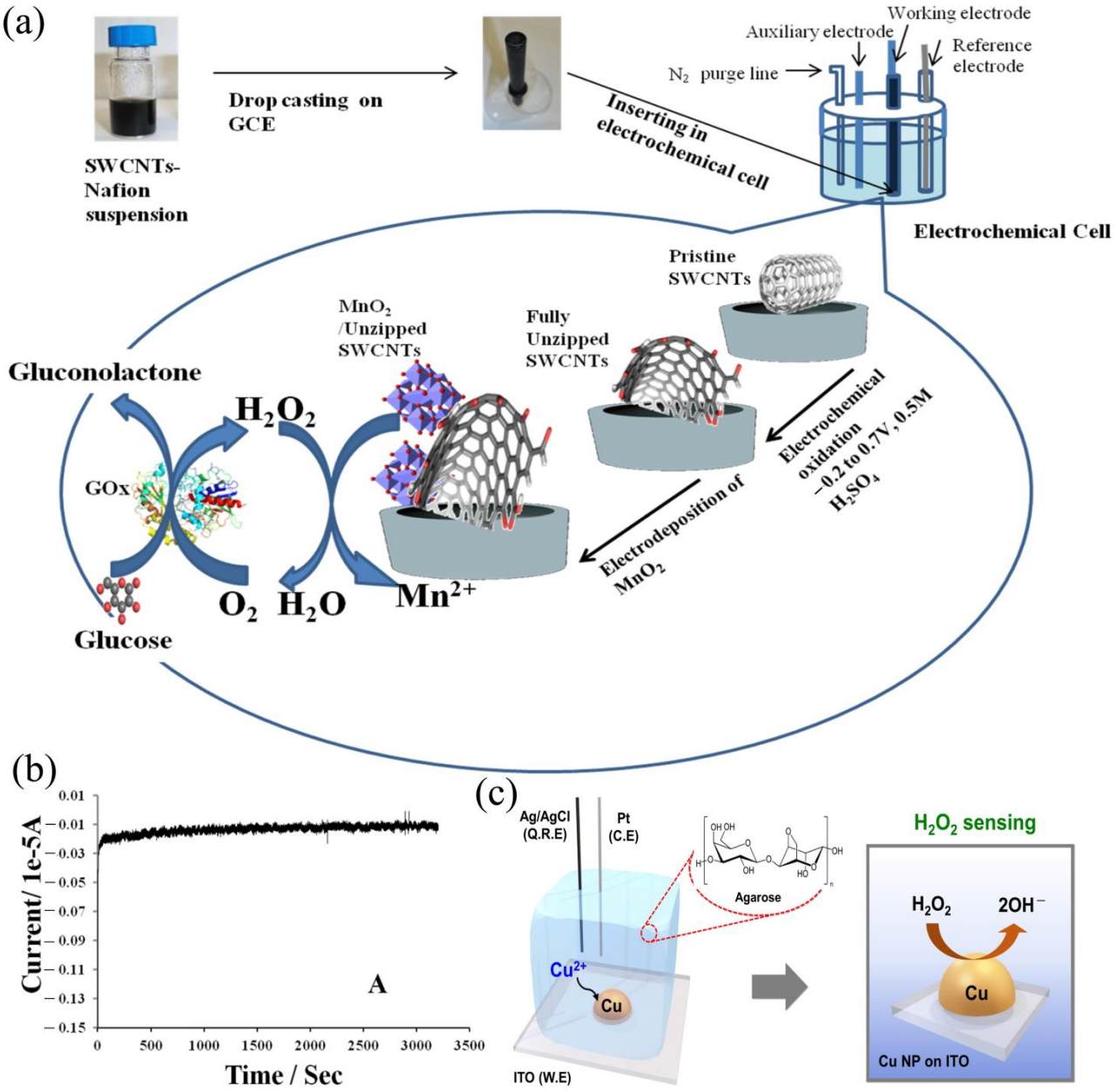

Figure 5. (**a**) The schematic diagram of the preparation and sensing mechanism and (**b**) the response stability of SWCNTs/MnO_2 based electrochemical sensor for solution-phase detection of H_2O_2 [61]. (**c**) The schematic diagram of the testing system and response mechanism of Cu NPs/ITO sensor for electrochemical detection of H_2O_2 [67].

Other innovative electrode designs include the use of Pt-treated pencil leads modified with o-phenylenediamine and phosphate-buffered saline for enhanced sensitivity (0.445 nA μM^{-1}) [91]. Cu^{2+}-exchanged zeolite has specific catalytic activity and ion exchange performance [92]. Cu^{2+}-exchanged zeolite combined with carbon paste electrodes (CPEs) has also been shown to accelerate H_2O_2 redox reactions, achieving high sensitivity (0.87 mA mol^{-1}) and detecting low concentrations (10 μM) [71]. Stoikov et al. [57] developed a screen-printed carbon electrode modified with carbon black, pillar[3]arene[2]quinone, and ferrocene, achieving a low LDL of 0.0003 μM and a linear detection range of 0.001 to 100 μM.

Compared to composite electrodes based on metal or metal oxides coated with carbon-based materials—which offer advantages such as excellent electrical conductivity, high chemical stability, a large specific surface area, and abundant availability—metal or metal oxides with specialized morphologies have also garnered significant attention in electrochemical sensing. Notably, NPs have been widely adopted in practical applications due to their straightforward preparation, high surface area, robust stability, and unique catalytic properties [93]. Ashraful Kader et al. [70] developed a composite electrode by blending Au NPs with SnO_2 nanofibers (NFs) and coating them onto a GCE. This Au NP/SnO_2 NF composite electrode demonstrated an impressive linear detection range for H_2O_2, spanning from 49.98 μM to 3937.21 μM. The Au NPs, acting as active sites, provided a peroxidase-like catalytic effect, enhancing the sensitivity, specificity, and selectivity of the H_2O_2 detection process by promoting the redox reaction. The sensor exhibited high sensitivity, reaching 14.157 μA mM^{-1}, indicating that even minor changes in H_2O_2 concentration could induce a substantial current response.

Bare ITO electrodes can also be modified with metal NPs to construct highly efficient H_2O_2 sensors through specialized preparation methods. For example, Han et al. [67] electrodeposited Cu NPs onto an ITO electrode using agarose hydrogel as a solid electrolyte. This approach provided a stable environment for the electrodeposition process and enhanced the mass transfer of copper ions, enabling selective electrochemical detection of H_2O_2 (Figure 5c). The resulting Cu NP/ITO sensor exhibited a wide linear detection range (1–500 μM) and achieved high sensitivity (0.0434 C μM^{-1}, where C represents charge) for H_2O_2 solutions. This method demonstrated good stability, reproducibility, and suitability for long-term monitoring in practical applications.

Further improvements in sensor response can be achieved by designing more diverse systems. Purwidyantri et al. [65] developed two types of active electrodes by coating ITO glasses with Au nanoframe arrays (GNA) and Au film-covered nanobeads (BGN) using a nanobead template method. The detection principle of H_2O_2 mainly involves three stages: the initiation of water electrolysis caused by surface electrode polarization, the autoionization of water, and the occurrence of an additional oxidation reaction when H_2O_2 is introduced to the interface. Interaction of H_2O_2 with the electrode interface induced additional oxidation reactions, leading to the production of hydrogen ions (H^+) and a corresponding decrease in local pH (Figure 6a). These pH changes were detected using electrochemical techniques such as ion-sensitive field-effect transistors (ISFETs) or cyclic voltammetry (CV). Among the electrodes, the GNA sensor demonstrated a strong linear relationship for H_2O_2 detection, covering a broad dynamic range from 10 to 100,000 μM, encompassing H_2O_2 concentrations relevant to most medical and environmental applications (Figure 6b,c).

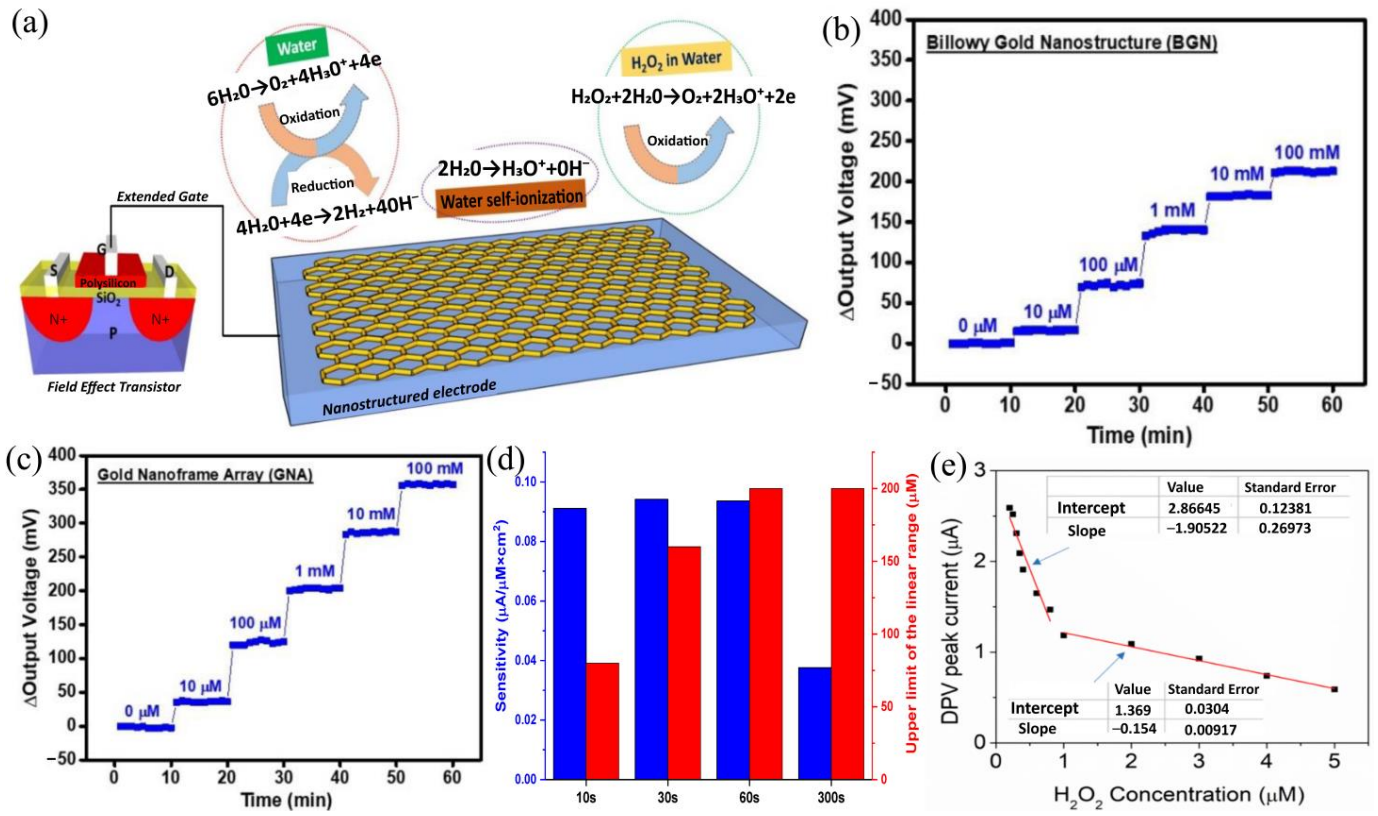

Figure 6. (**a**) The H_2O_2 solution detection mechanism of BGN and GAN extended-gate field-effect transistor electrode, and the application of (**b**) BGN and (**c**) GAN electrode in real-time detection of H_2O_2 [65]. (**d**) The sensitivity and linearity rang of TiO_2 NTs activated by different self-doping times [63]. (**e**) The peak current of DPV changes of Te NSs based H_2O_2 sensor [62].

Further modification of metal oxide materials can significantly enhance their performance as sensing electrodes. For instance, doping TiO_2 nanotubes (NTs) has proven to be an effective strategy for tailoring their physical and chemical properties to meet specific application requirements [94]. Doping enhances charge carrier dynamics, optimizes the band structure, and increases the catalytic activity of TiO_2 NTs, thereby improving their performance in electroanalysis and photocatalysis [95]. Spanu et al. [63] demonstrated the electrochemical self-doping of TiO_2 nanotubes in ethylene glycol (EG) electrolyte under varying voltages and treatment times. The sensitivity and linear detection range of the self-doped TiO_2 NTs improved significantly with increasing treatment time (Figure 6d). Notably, at a treatment time of 60 s and a voltage of −1.5 V, the sensitivity of the TiO_2 NTs towards H_2O_2 solutions was markedly enhanced. The sensor exhibited a good linear response across a wide detection range (3–200 μM) for H_2O_2 concentration. This improvement is attributed to the formation of Ti^{3+} sites on the NT surfaces during the doping process. These sites act as electron traps, facilitating charge separation and transport, thereby enhancing the electrochemical activity for the sensitive detection of H_2O_2.

In recent years, electrochemical biosensors based on biological recognition elements, such as those modified with horseradish peroxidase (HRP), have made significant progress. These sensors exhibit excellent selectivity, biocompatibility, and high sensitivity, enabling the detection of very low concentrations of H_2O_2 [96–98]. However, enzyme-based biosensors have certain limitations, including susceptibility to temperature and pH variations, as well as potential toxic effects on enzyme activity from interfering substances [99]. To address these issues, non-enzymatic electrochemical methods have emerged as a research hotspot [100]. For example, Shringi et al. [62] developed a non-enzymatic sensor by using a

simple ultrasonic method to mix two-dimensional (2D) tellurium (Te) nanosheets (NSs), characterized by their high specific surface area and excellent electrochemical performance, with a chitosan solution. The resulting composite was drop-coated onto a GCE to form the sensor. This composite electrode demonstrated a significant and linear current response to H_2O_2 concentrations, achieving an LDL of 0.47 μM and a sensitivity of 27.2 μA μM^{-1} cm^{-2} (Figure 6e). On the electrode surface, Te NSs engaged in electrochemical redox reactions with H_2O_2, generating a measurable current signal proportional to the H_2O_2 concentration. Compared to traditional enzymatic sensors, this non-enzymatic sensor offers superior stability and durability, making it well-suited for long-term monitoring in practical applications. This advancement underscores the potential of non-enzymatic methods to overcome the inherent limitations of enzyme-based biosensors.

Luo et al. [69] prepared laser-scribed graphene (LSG) electrodes by laser etching on polyimide (PI) films, using TMB as a substrate. HRP catalyzes the oxidation of TMB by H_2O_2 to generate a current signal, thereby enabling the detection of H_2O_2. Furthermore, the LSG electrochemical sensing platform was integrated with a smartphone to achieve portable and remote monitoring. Its linear range is 20–3400 μM and its LDL is 4.6 μM.

Guo et al. [59] developed an electrochemical platform based on organic electrochemical transistors (OECTs). This platform was constructed using a flexible polyethylene terephthalate substrate and a Transwell support. Screen-printed CPEs, modified with multi-walled carbon nanotubes (MWCNTs) and Pt NPs, were employed as the gate electrode for the OECT. By analyzing the electrochemical response of OECTs to H_2O_2, the concentration of H_2O_2 could be determined by measuring changes in gate voltage and drain-source current. This method enabled detection within an H_2O_2 concentration range of 0.5 μM to 100 μM, with an LDL of 0.2 μM. For rapid and highly sensitive monitoring of trace amounts of H_2O_2, Lee et al. [56] utilized a graphene field-effect transistor (FET) modified with cytochrome C (Cyt c). When Cyt c interacts with H_2O_2, its oxidation state changes, inducing a charge on the surface of graphene, which alters the FET's drain-source current. By measuring these current changes in real-time, the H_2O_2 concentration could be monitored with an exceptional LDL of 100 fM and a detection range of 100 pM to 100 fM, demonstrating remarkable sensitivity.

Modified electrodes are commonly employed as signal transducers in electrochemical sensors. These electrodes can distinguish signals from analytes with similar redox potentials, amplify current responses, reduce the overpotentials of electrode reactions, and facilitate analyte accumulation [101]. However, multilayer deposition and complex compositions can complicate sensor fabrication and reduce compatibility between modifiers and substrates [102]. Additionally, in real-world applications, the small redox potential differences of structural analogs can lead to peak overlap, limiting the selectivity of these sensors.

The stability and durability of working electrodes are crucial for the service life of electrochemical sensors. Over time, sensors may experience degradation or contamination of the electrodes, leading to reduced performance. Although electrochemical chemosensors have made significant advances in H_2O_2 detection, further efforts are required to optimize material systems, improve composite interface properties, enhance outer interface adsorption and interaction with H_2O_2, and develop new active electrodes or innovative preparation methods. Combining electrochemistry with other detection principles offers a promising pathway for advancement [103].

For instance, Fagadar-Cosma et al. [50] synthesized Pt(II)-5,10,15,20-tetra(4-allyloxyphenyl) porphyrin (TAPP) and bonded it onto the surface of polydimethylsiloxane to create a dual-channel sensor for H_2O_2. This fluorescence-electrochemical sensor demonstrated rapid response, low LDL (0.03 μM), and good repeatability (Figure 7a). At the same time, this dual-channel detection method expands the detection range (1–50 μM).

Another promising approach is the integration of chemiluminescence and electrochemistry, resulting in electrochemiluminescence immunoassay (ECLIA) technology [104]. ECLIA has been widely adopted in clinical laboratories due to its advantages, including the absence of an external light source, spatial control of radiation, and a high signal-to-noise ratio. This technology is particularly attractive for biological analyses targeting antigens or antibodies. Its selectivity can be further enhanced by adjusting electrode potentials to control the substances oxidized/reduced at the electrode and involved in surface reactions. Such advancements highlight the potential for combining complementary techniques to achieve more sensitive, selective, and durable electrochemical sensors for H_2O_2 detection.

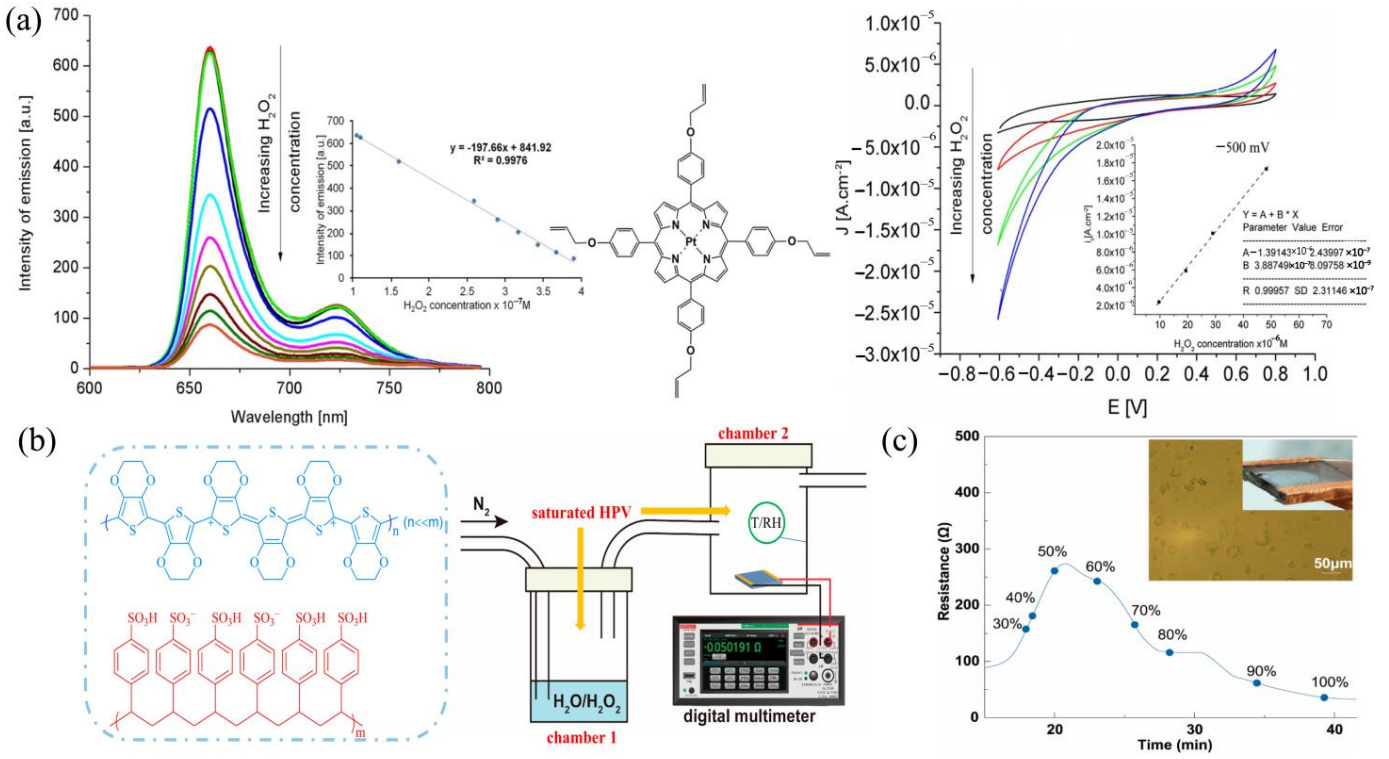

Figure 7. (**a**) The molecular structure of TAPP and the results of Pt(II)-TAPP sensor for fluorescent and electrochemical detection of H_2O_2 [50]. (**b**) The molecular structure of PEDOT:PSS, a schematic diagram of the testing system for detecting H_2O_2 vapor on the basis of PEDOT:PSS/PEDOT film sensor, and (**c**) its resistance change under different environmental humidity [73].

2.2.2. Chemiresistive Sensor

Compared to electrochemical methods, chemiresistive sensors have gained significant attention due to their simpler operation and cost-effectiveness. These sensors do not require electrochemical workstations or complex multi-electrode systems, making them more accessible for practical applications. As an example, our group developed a poly(3,4-ethylenedioxythiophene):polystyrene sulfonate (PEDOT:PSS)/PEDOT film through in-situ electrochemical polymerization of the 3,4-ethylenedioxythiophene (EDOT) monomer on a PEDOT:PSS substrate. This chemiresistive sensor exhibited an initial resistance of 87 Ω and successfully detected H_2O_2 vapor at room temperature (Figure 7b) [73]. For low-concentration H_2O_2 vapor (1.0 ppm), the sensor demonstrated a continuous increase in electrical resistance over time. Notably, the sensor remained functional in a high-humidity environment, with relative humidity increasing from 25% to 100% during the detection process (Figure 7c). This ability to operate in humid conditions addresses a critical challenge for gas sensors, where humidity often acts as a major interference factor.

Intrinsically conductive polymers (ICPs), such as PEDOT:PSS and PEDOT, were chosen for their unique electrical, optical, mechanical, and surface-interface properties, including adsorption and wettability. Their commercial availability and stability further enhance their suitability for gas detection applications. Building on this, we also developed a dual-signal sensing film, PEDOT:PSS-ammonium titanyl oxalate (ATO)/PEDOT, which combines colorimetric and chemiresistive responses [74]. This film detected H_2O_2 vapor at room temperature within a range of 1.0–10.5 ppm, accompanied by a visible color change from blue to yellow-green. However, the overall performance of chemiresistive sensors still lags behind that of optical and electrochemical detection methods. Challenges such as long-term material stability, signal reliability, and the coordination mechanisms of dual or multiple signals require further investigation. Continued efforts are essential to optimize chemiresistive sensor systems and unlock their full potential for H_2O_2 detection.

3. Applications of Chemosensors for H_2O_2 Detection

Currently, chemosensors for liquid- and gas-phase H_2O_2 detection, utilizing various response principles, have demonstrated wide-ranging applications across numerous fields [105–107]. These sensors offer a combination of advantages, including high sensitivity, fast response, and good stability, along with simplicity in technology, equipment accessibility, and cost-effectiveness compared to methods like chromatography. Such attributes enable effective monitoring of H_2O_2 concentrations, ensuring safety and health in vivo and in vitro environments or maintaining the operational safety and effectiveness of processes such as H_2O_2 disinfection [108]. In this section, we introduce and analyze representative applications of H_2O_2 chemosensors across four key areas: food inspection, environmental and safety monitoring, disease surveillance, and plant status monitoring [109–111].

3.1. Food Inspection

The food industry represents a major application area for H_2O_2, where it is frequently used as a food-grade additive for bleaching, preservation, or accelerating fermentation. Additionally, H_2O_2 serves as a disinfection and sterilization agent for production equipment, pipelines, containers, packaging materials, production spaces, and even food production personnel [107,112]. In this context, chemosensors play a vital role by monitoring residual H_2O_2 levels in food or during production processes in real-time, ensuring safe and hygienic practices to protect the health of both consumers and producers [105]. For instance, to enable rapid and accurate detection of trace amounts of H_2O_2 in complex food matrices (e.g., milk), Oliveira et al. [113] developed a modified polypyrrole (PPy)-MN electrode. This electrochemical sensor was constructed by integrating magnetite Fe_3O_4 nanoparticles with the conducting polymer PPy and polysaccharides (cashew gum polysaccharide, CGP). The residual amount of H_2O_2 in milk must not exceed a certain limit (0.0147 mM). The sensor demonstrated an effective amperometric response and was successfully applied to detecting H_2O_2 in food matrices such as milk (5.6×10^{-5} μA mM^{-1}) and skimmed milk (1.7×10^{-4} μA mM^{-1}) (Figure 8a).

Compared to electrochemical analysis, colorimetric detection of H_2O_2 is also widely used in food quality and safety testing due to its simplicity and visual detectability. For example, Baye et al. [33] synthesized a porous and nanostructured Fe_3O_4-Fe^0/Fe_3C nanozyme, which was employed as a peroxidase mimic for the colorimetric detection of H_2O_2. This nanozyme demonstrated a remarkably low LDL of 67.1 pM and exhibited excellent recovery rates (99.8–101.6%) when a known concentration of H_2O_2 was added to milk samples. Additionally, its low relative standard deviation indicated high accuracy.

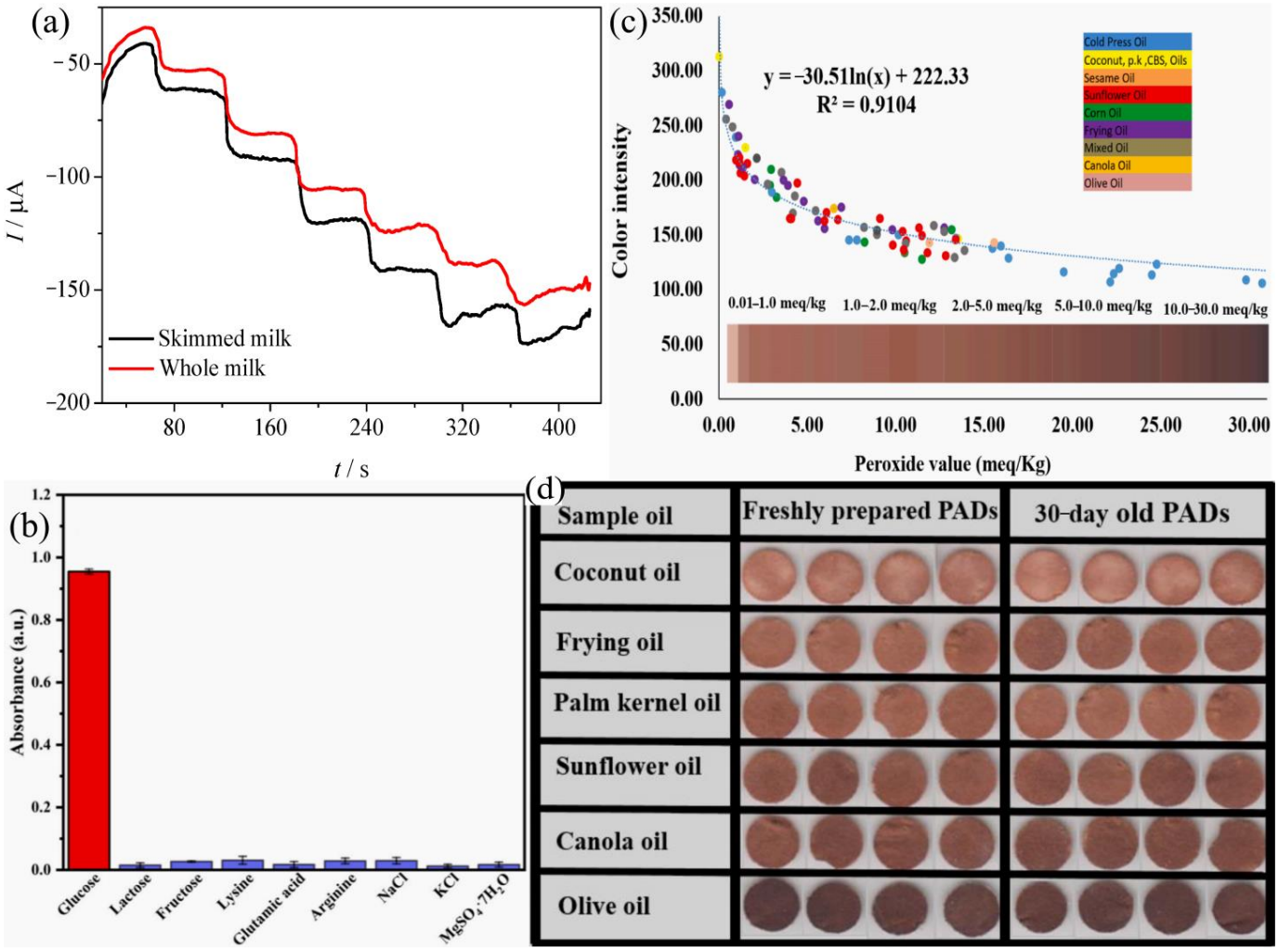

Figure 8. (**a**) The amperometric response of modified electrode containing PPy(CGP)-MN toward H_2O_2 (1 mmol/L) in whole milk and skimmed milk [113]. (**b**) The selective detection of glucose by $CoCO_3$/TMB sensor in the presence of a variety of interfering substances [38]. (**c**) The color intensity (brown) detected by PAD as compared with the official method, and (**d**) the color morphology of fresh vegetable oil samples as compared with the corresponding samples after 30 days of storage [46].

To detect residual H_2O_2 in soaked foods, Wu et al. [47] fabricated boron- and phenyl-doped graphitic carbon nitride nanosheets (BPCN NSs) as a colorimetric sensor. Chicken claws were soaked in H_2O_2 solutions with concentrations of 1.3%, 2%, 5%, and 10% for 3 h to simulate real-world conditions. The BPCN NSs sensor demonstrated high sensitivity and selectivity for detecting H_2O_2 residues at low concentrations (1.3% and 2%) in chicken feet, which conventional potassium permanganate titration methods failed to detect.

In addition, H_2O_2 can serve as an indicator and medium for assessing the content of other food-derived components. For instance, to address the simultaneous detection of H_2O_2, glucose, and ascorbic acid, Peng et al. [38] synthesized a $CoCO_3$ nanozyme with peroxidase-like activity. This nanozyme catalyzed the oxidation of the chromogenic substrate TMB in the presence of H_2O_2, resulting in a color change from light blue to dark blue. Using this property, glucose oxidase (GOx) was employed to catalyze the oxidation of glucose to produce H_2O_2. The $CoCO_3$ nanozyme then catalyzed the oxidation of TMB by the generated H_2O_2, causing a distinct color change. This process enabled the colorimetric detection of glucose. The method demonstrated good anti-interference properties against various substances, including sugars, amino acids, and metal ions (Figure 8b). Moreover, it was successfully applied to detect glucose levels in sugar-free beverages available on the

market, such as energy drinks, grape bubble drinks, and sparkling water. The recovery rates ranged from 92.9% to 105.5%, indicating the method's high accuracy and reliability.

On the other hand, the oxidation level of vegetable oils can be evaluated by measuring their peroxide value (PV), an important parameter used to monitor oil quality and safety [114]. Ghohestani et al. [46] developed a colorimetric detection method using a paper-based analytical device (PAD) to enable rapid, simple, low-cost, and visual detection of PV. In this approach, lipid peroxides in the oil react with potassium iodide (KI) to produce iodine, which subsequently reacts with starch to form a blue-colored complex. The intensity of the color is directly proportional to the PV (Figure 8c). This method was applied to detect PV in various vegetable oil samples, including corn oil, sesame oil, sunflower seed oil, frying oil, mixed oil, coconut oil, palm kernel oil, and cocoa butter substitutes. The results were highly consistent with those obtained using the standard method, with errors remaining within the acceptable range. Furthermore, after 30 days of storage, the detection results showed no significant differences (Figure 8d), demonstrating the good stability of this sensor. The simplicity of operation and the lack of a need for complex instruments make this method particularly suitable for rapid on-site detection of both solid and liquid vegetable oils.

3.2. Environmental and Safety Monitoring

H_2O_2 has broad applications and significant value in environmental and safety fields, including wastewater treatment, air purification, soil remediation, chemical production, and medical procedures [14,15]. However, excessive use or residual pollution of H_2O_2 poses risks to environmental and public safety. Chemosensors play a vital role in the sensitive and selective detection of H_2O_2, helping to avoid overuse, monitor pollution levels, and identify risk factors such as explosive threats in public places. These sensors enable real-time monitoring of H_2O_2 concentrations in wastewater, air, soil, and other media.

In environmental monitoring and assessment, timely and accurate detection of H_2O_2 concentrations provides essential insights into pollution levels, helps identify potential risks early, and protects ecological health [115,116]. For instance, Zhang et al. [37] developed a colorimetric biosensor using HRP and $Cu_3(PO_4)_2 \cdot 3H_2O$ as organic and inorganic components, respectively, via a one-pot incubation method. This sensor employed a smartphone camera to capture color changes, which were analyzed using dedicated software to quantify H_2O_2 concentrations (Figure 9a). It demonstrated a wide detection range of 5–500 μM, high sensitivity, and excellent anti-interference properties, with an associated error of approximately 1%. The sensor successfully detected H_2O_2 concentrations as low as 20 μM in real-world scenarios. In another study, Kumar et al. [45] used colloidal AgNPs to develop a method for the selective colorimetric detection of H_2O_2 in environmental samples, such as river and tap water. The sensor system demonstrated high accuracy and sensitivity, detecting H_2O_2 concentrations as low as 0.216 ppm with a recovery rate of 99%. These advancements highlight the potential of chemosensors to address critical challenges in environmental and safety monitoring effectively.

Vahidpour et al. [117] developed a novel biosensor for detecting low concentrations of H_2O_2 vapor/aerosol by utilizing HRP as the enzyme and an interdigital electrode structure. The biosensor demonstrated a rapid response time of less than 60 s for concentrations up to 630 ppm. The sensor's performance was evaluated in a simulated medical/pharmaceutical isolator environment using a glass box setup. It exhibited excellent sensitivity and stability, accurately detecting low concentrations (<110 ppm) of H_2O_2 vapor/aerosol, making it a promising tool for real-time monitoring in pharmaceutical and medical environments.

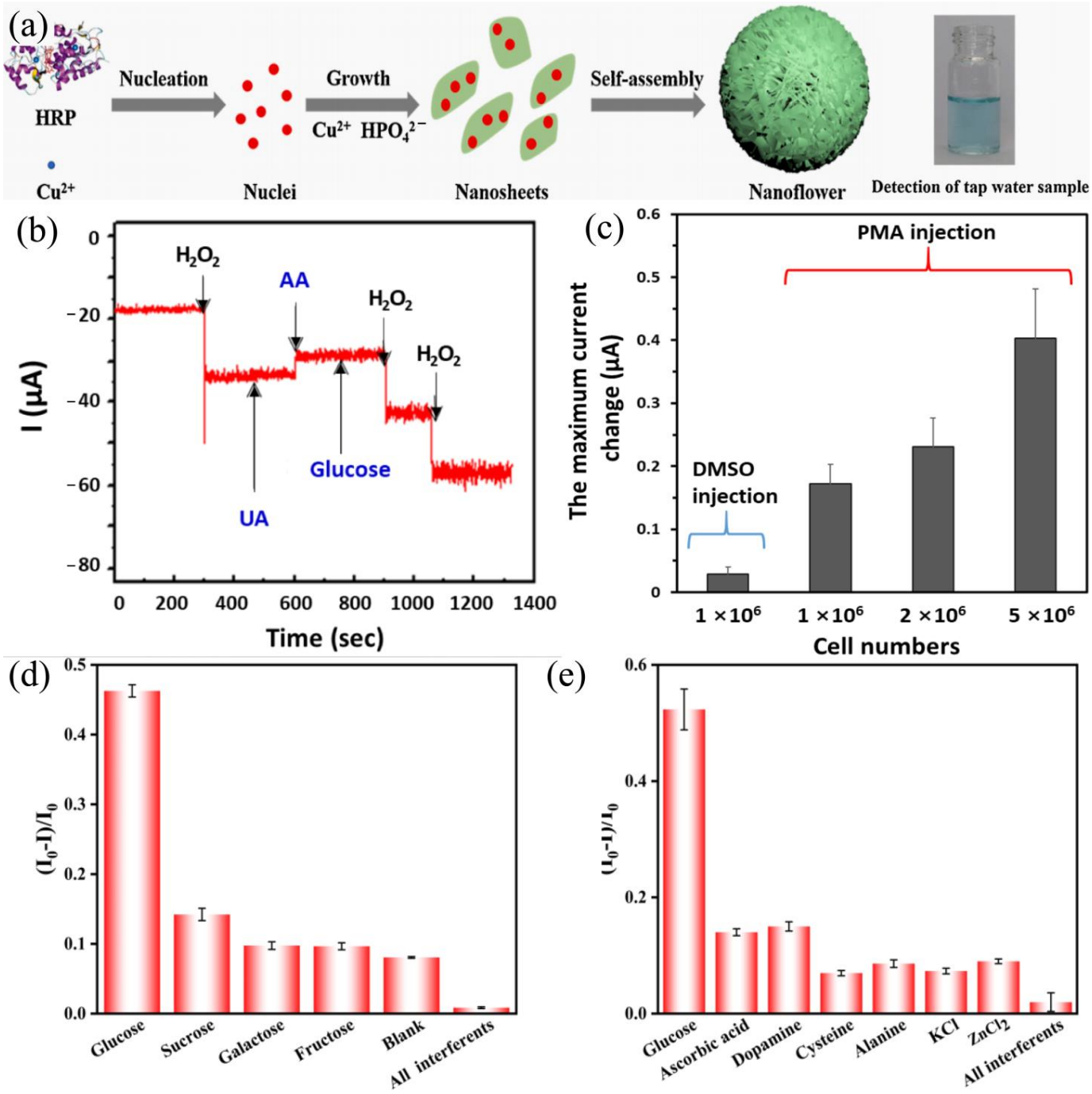

Figure 9. (**a**) Synthesis schematic of HRP/$Cu_3(PO_4)_2 \cdot 3H_2O$ hybrid nanoflowers [37]. (**b**) Electrical current changes observed in the presence of AA, UA, and glucose, and (**c**) changes in cell number after injection of DMSO and PMA [68]. Sensitivity changes of glucose as detected in (**d**) buffer and (**e**) diluted serum [60].

In the field of safety identification, the measurement of H_2O_2 vapor is crucial in scenarios involving its production, storage, and use [118]. In a normal working environment, the safe concentration of hydrogen peroxide should not exceed 0.92 mM. For example, Romolo et al. [119] explored the on-site detection and analysis of H_2O_2 vapor using an HRP- and luminol-based chemiluminescence sensor in both indoor and outdoor environments. This sensor achieved an LDL of 0.2 μM in indoor settings. Additionally, detecting volatile organic compounds and small molecule oxidizers such as H_2O_2 is critical for ensuring public safety and preventing explosion accidents. Many flammable and explosive volatile

compounds release oxidizing gas molecules, providing opportunities for detection through specialized gas chemosensors. However, different explosives emit distinct volatile gas components at varying concentration ranges, presenting significant challenges to the sensitivity and accuracy of these sensors. Given the complexity of gas-phase applications, there is currently no internationally defined concentration limit for H_2O_2 vapor, and reaching a consensus on this matter remains a future goal. Developing advanced gas-phase chemosensors with improved sensitivity and accuracy will be vital for addressing these challenges and enhancing safety monitoring systems.

3.3. Disease Surveillance

Beyond its common uses in disinfection, sterilization, and bleaching of medical instruments and hospital environments, studying the role of H_2O_2 in biological processes is of critical importance. As a key ROS in organisms, the concentration of H_2O_2 is closely linked to various physiological and pathological processes [120–122]. Changes in H_2O_2 levels in biological samples (such as blood, urine, and tissue fluid) are often associated with the onset and progression of diseases, including cancer, inflammation, and oxidative stress [42,64,68]. Accurate measurement of H_2O_2 concentrations is essential to ensure biomedical accuracy and reliability, necessitating the use of highly sensitive, precise, and stable sensors. These sensors provide valuable insights into the complex roles of H_2O_2 in health and disease, supporting advancements in diagnostics and therapeutic interventions.

Chemosensors, particularly those based on electrochemical principles, are widely utilized for H_2O_2 detection due to their high sensitivity, rapid response, and easy integration [123]. Cancer cells produce higher levels of ROS than normal cells, with H_2O_2 concentrations increasing as tumors grow [23]. Lee et al. [68] developed an electrochemical sensor using a screen-printed carbon electrode (SPCE) modified with PtNPs and reduced graphene oxide-carbon nanotube (rGO-CNT) nanocomposites. This PtNP/rGO-CNT/PtNP/SPCE sensor demonstrated a strong linear response to H_2O_2 concentrations ranging from 25 to 1000 μM. The sensor exhibited high sensitivity to H_2O_2 compared to common interfering substances such as ascorbic acid (AA), uric acid, and glucose (Figure 9b). It effectively distinguished between H_2O_2 released by unstimulated and stimulated prostate cancer cells (LNCaP). Upon stimulation of LNCaP cells with dimethyl sulfoxide (DMSO) and 12-myristate 13-acetate (PMA), a significant current change was observed, indicating increased H_2O_2 release (Figure 9c).

Wiedemair et al. [64] designed an amperometric sensor to monitor exhaled H_2O_2 in both static and flow modes. An agarose layer was employed as an enrichment membrane to enhance the uptake of gaseous H_2O_2, ensuring reliable gas-phase detection. In the flow setting, the sensor detected H_2O_2 concentrations as low as 42 ppb within 5 min, showcasing a low limit of detection. Yu et al. [42] developed a dual-mode sensing platform for in-situ H_2O_2 detection in living cells. This portable colorimetric-electrochemical sensor, based on MOF-818 nanozymes, enabled the simultaneous detection of H_2O_2 and H_2S released by stimulated HeLa cells. By combining the advantages of colorimetric and electrochemical methods, this platform improved the accuracy and reliability of biomedical detection, offering a versatile tool for studying dynamic ROS changes in biological systems.

As mentioned earlier, glucose plays a vital role in clinical diagnostics and medical research [123]. The colorimetric determination of glucose concentration using H_2O_2 as an intermediary is particularly important for diagnosing and managing various diseases [124]. For instance, Zheng et al. [60] utilized AuNPs to catalyze the oxidation of glucose by GOx, producing H_2O_2. A series of chemical reactions then altered the aggregation state of AuNPs, enabling the colorimetric detection of glucose in diluted serum samples. The recovery of glucose ranged from 81.1% to 118%, with relative standard deviations of 1.42% to 1.98% (Figure 9d,e). Similarly, Wu et al. [35] synthesized AgNPs@MOF nanozymes, leveraging their peroxidase-like activity for the selective colorimetric detection of glucose. This method effectively distinguished glucose from other sugars such as sucrose, galactose, and fructose. The sensor exhibited an LDL of 0.17 μM, demonstrating potential for diabetes monitoring. Both enzymatic and non-enzymatic sensors can be used for the detection of glucose and are suitable for glucose concentration monitoring in physiological liquids. However, the enzymatic sensor has a stronger anti-interference ability to interfering substances and is suitable for long-term monitoring applications [125].

In the human body, blood glucose is enzymatically converted to gluconic acid, releasing H_2O_2 as a byproduct [126]. Therefore, the concentration of glucose can be indirectly inferred by detecting H_2O_2 levels [127]. Xu et al. [58] developed a Fe_3O_4@MoS_2-AuNP composite sensor, combining the peroxidase activity of Fe_3O_4 with the electrochemical activity of AuNPs. This dual-mode sensor enabled both colorimetric and electrochemical detection of H_2O_2 with an LDL as low as 0.08 μM. For real human serum samples, the recovery rates of H_2O_2 were 95.03–108.06% in the colorimetric mode and 87.55–113.13% in the electrochemical mode, showcasing its high accuracy and reliability.

Colorimetric methods have also been applied to the direct detection of H_2O_2 in plasma. For instance, Parveen et al. [36] synthesized RuO_2 quantum dots (QDs) with high stability and excellent water dispersibility, using proteins released by *Fusarium oxysporum* as capping agents. The high oxidative capacity of H_2O_2 oxidized the RuO_2 QDs, resulting in the formation of their respective oxidation products. This process led to a significant decrease in the absorption peak at 400 nm, accompanied by a visible color change from yellowish grey to pale yellow and eventually to colorless. When the ratio of RuO_2 QDs to H_2O_2 was 9:1, the method achieved a low LDL of 0.39 μM, demonstrating high sensitivity and feasibility for detecting H_2O_2 in plasma samples (Figure 10a).

The detection of H_2O_2 can also serve as an indicator for evaluating organ health, particularly liver function [128]. In cases of drug-induced injury, H_2O_2 is endogenously produced in the liver. Xu et al. [34] developed a dual-mode colorimetric and fluorescent probe, XH-2 (Φ_F = 0.15), by grafting boric acid as a specific recognition group onto the fluorophore XH-1 (Φ_F = 0.34) (Figure 10b). This design provides high sensitivity and selectivity for H_2O_2 detection. The probe can detect H_2O_2 levels in cells and distinguish different concentrations ranging from 0 to 120 μM. This capability enables the monitoring and assessment of drug-induced hepatotoxicity, such as that caused by acetaminophen, by observing changes in H_2O_2 levels (Figure 10c).

Nevertheless, while single-mode or dual-mode chemosensors are capable of providing real-time monitoring of H_2O_2, their use in disease diagnosis often requires integration with other methods, such as biochemical analysis or imaging examinations. This combination ensures comprehensive judgment, enhancing the accuracy and reliability of diagnostic outcomes.

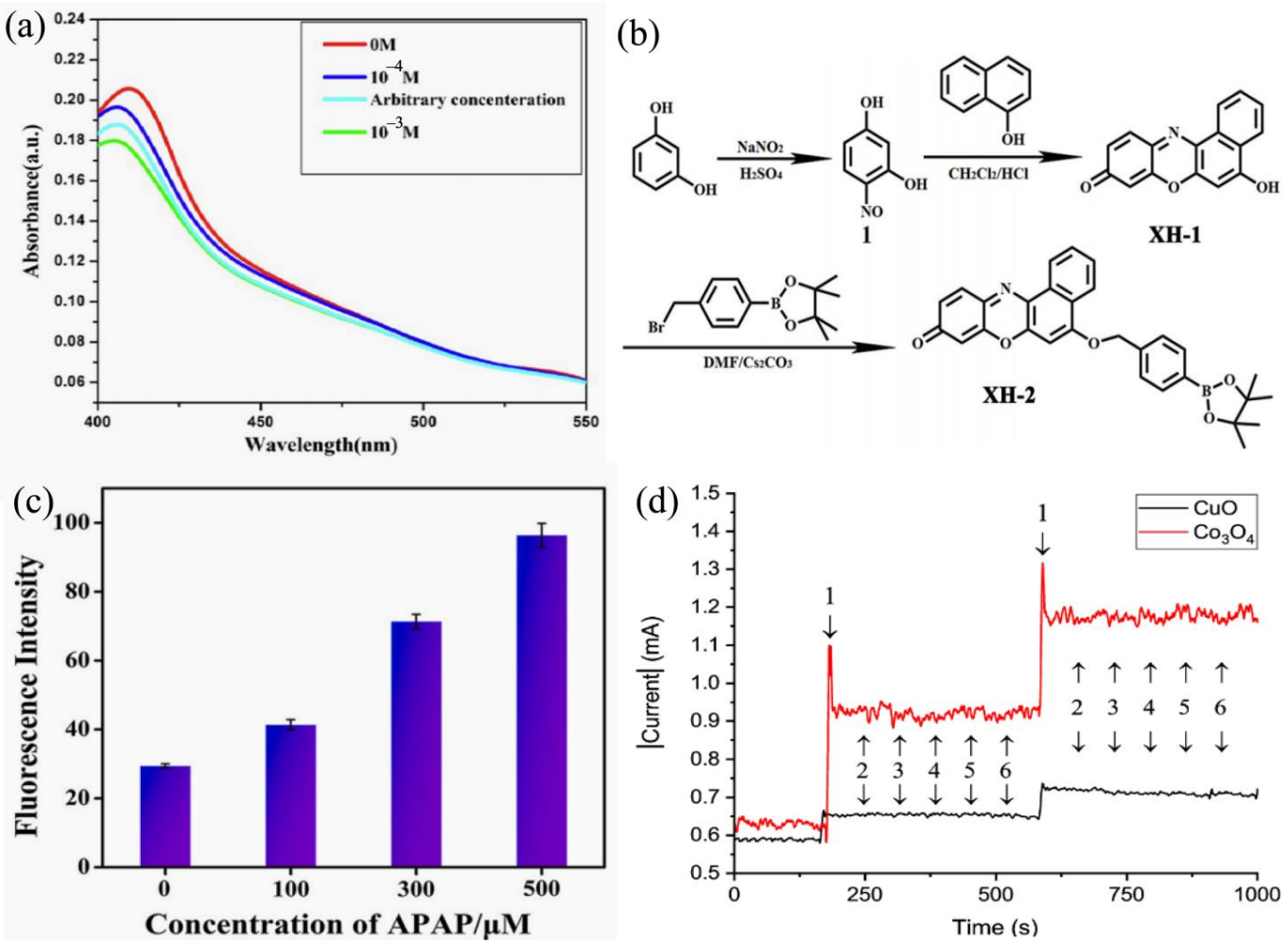

Figure 10. (**a**) UV-Vis absorption spectra of RuO_2 QDs before and after adding 0–10^{-3} M H_2O_2 to the plasma [36]. (**b**) Preparation process of probe XH-2. (**c**) The fluorescence intensity of HepG2 cells treated with different concentrations of APAP and probe XH-2 [34]. (**d**) The signal response of H_2O_2 (1) in comparison to the potential interfering substances NaCl (2), KNO_3 (3), glucose (4), citric acid (5), and ascorbic acid (6) as tested for the CuO and Co_3O_4 sensors [66].

3.4. Plant Status Monitoring

H_2O_2 has extensive applications in plants, including promoting growth, disinfection, sterilization, disease prevention, pest control, and weed removal. Additionally, H_2O_2 serves as an important signaling molecule, playing a crucial role in assessing plant status [129]. It regulates various processes related to plant growth and development, such as root elongation, stomatal closure, and leaf expansion. By influencing the synthesis and distribution of plant hormones, H_2O_2 significantly impacts plant growth patterns [130]. However, it is essential to carefully manage H_2O_2 concentration, timing of application, and safety, as excessive exposure can harm plant cells. For example, Mihailova et al. [66] developed electrochemical sensors based on nanostructured CuO and Co_3O_4 to detect H_2O_2 in rye samples, aiming to evaluate oxidative stress in plant tissues. The sensitivity and LDL of CuO and Co_3O_4 electrodes were 439.19 μA mM^{-1} with 1.34 μM and 505.11 μA mM^{-1} with 1.05 μM, respectively. The CuO/Co_3O_4 sensor demonstrated high selectivity for H_2O_2, effectively eliminating interference from common substances such as NaCl, KNO_3, glucose, citric acid, and AA (Figure 10d).

4. Conclusions

As summarized in Table 1, chemosensors for H_2O_2 detection have achieved remarkable progress in recent years, leveraging innovative materials, diverse sensing mechanisms, and expanded application fields. Selecting an appropriate detection method requires careful consideration of the detection medium (liquid, solid, or vapor phase), specific needs, and conditions to ensure accuracy and reliability.

The introduction of advanced materials, such as functional graphene, nanostructured metals or metal oxides, conductive polymers (CPs), and novel post-treatment techniques, has significantly improved the sensitivity and stability of conventional H_2O_2 chemosensors. Additionally, nano-catalysts and biocatalysts, such as enzymes with catalytic properties, enhance both the selectivity and sensitivity of H_2O_2 sensors. As an intermediary, H_2O_2 detection also provides opportunities for detecting biological components and diagnosing diseases.

However, current chemosensors often struggle to meet the accuracy and reliability required for detecting low H_2O_2 concentrations. Transitioning from single-mechanism to multi-mechanism responses, particularly combining optical and electrical modes, holds promise for future advancements. Developing moisture-resistant probing materials is also critical for reliable gaseous sensors. The stability of chemosensors is paramount for ensuring long-term viability, as high H_2O_2 concentrations can lead to oxidative degradation and interactions with moisture that compromise sensing material systems. Consequently, careful development of organic sensing materials is necessary.

Looking ahead, advances in material science, nanotechnology, and biotechnology are expected to drive the emergence of more efficient H_2O_2 chemosensors. These future sensors will likely integrate intelligent features, such as automatic calibration, self-diagnosis, and remote monitoring, improving convenience and reducing human error. Market competition and manufacturing advancements will further drive cost reductions and maintainability improvements through the use of low-cost materials and optimized production processes. The potential for miniaturization and integration of chemosensors into portable devices, such as smartphones or wearable devices, is particularly exciting. With microelectronics technology, H_2O_2 chemosensors could provide real-time monitoring and simultaneously detect multiple gases through multi-sensor systems. These innovations will make H_2O_2 detection more accessible and practical for a variety of applications.

In conclusion, the future of H_2O_2 chemosensors lies in miniaturization, intelligence, and multifunctionality. These developments will meet the needs of diverse domains while emphasizing simplicity, practicality, and cost-effectiveness. Moreover, emerging applications—such as controlled concentration release in H_2O_2-based hydrogen storage, photocatalytic production or degradation, and sterilization—highlight the potential for linking H_2O_2 sensing with new technological frontiers. These advancements promise a broader and brighter future for H_2O_2 chemosensor technology.

Author Contributions: M.Z. organized and wrote the manuscript. H.S., M.Y., R.D. and X.Y. revised and formated the manuscript. S.C. and L.Z. supervised and proposed the review topic and its outline, wrote and revised the manuscript. All authors have read and agreed to the published version of the manuscript.

Funding: The financial support from the National Natural Science Foundation of China (No. 32360620) and the Academic Development Project of TongXin Funds (No. 2024161815) is gratefully acknowledged.

Institutional Review Board Statement: Not applicable.

Informed Consent Statement: Not applicable.

Conflicts of Interest: The authors declare no conflict of interest.

References

1. Rampon, C.; Volovitch, M.; Joliot, A.; Vriz, S. Hydrogen peroxide and redox regulation of developments. *Antioxidants* **2018**, *7*, 159. [CrossRef] [PubMed]
2. Ciriminna, R.; Albanese, L.; Meneguzzo, F.; Pagliaro, M. Hydrogen peroxide: A key chemical for today's sustainable development. *ChemSusChem* **2016**, *9*, 3374–3381. [CrossRef]
3. Chen, Y.; Zaman, F.; Jia, Y.; Huang, Y.; Li, T.; Bai, F.; Song, L.; Li, J. Harmful cyanobacterial bloom control with hydrogen peroxide: Mechanism, affecting factors, development, and prospects. *Curr. Pollut. Rep.* **2024**, *10*, 566–579. [CrossRef]
4. Rigoletto, M.; Laurenti, E.; Tummino, M.L. An overview of environmental catalysis mediated by hydrogen peroxide. *Catalysts* **2024**, *14*, 267. [CrossRef]
5. Ullah, N.; Khan, S.; Barton, B.; Guziejewski, D.; Smarzewska, S.; Koszelska, K.; Mirceski, V. A mini review on topographical and structural insight of metal carbides for electrocatalytic hydrogen peroxide detection. *Microchem. J.* **2024**, *200*, 109961. [CrossRef]
6. Xing, L.; Zhang, W.; Fu, L.; Lorenzo, J.M.; Hao, Y. Fabrication and application of electrochemical sensor for analyzing hydrogen peroxide in food system and biological samples. *Food Chem.* **2022**, *385*, 132555. [CrossRef] [PubMed]
7. Pirsa, S.; Purghorbani, F. An overview of hydrogen peroxide sensors and their applications in food quality control. *Sens. Rev.* **2024**, *44*, 159–170. [CrossRef]
8. Winterbourn, C.C. Biological production, detection, and fate of hydrogen peroxide. *Antioxid. Redox Signal.* **2018**, *29*, 541–551. [CrossRef] [PubMed]
9. Burek, B.O.; Bormann, S.; Hollmann, F.; Bloh, J.Z.; Holtmann, D. Hydrogen peroxide driven biocatalysis. *Green Chem.* **2019**, *21*, 3232–3249. [CrossRef]
10. Ruan, S.; Liu, W.; Wang, W.; Lu, Y. Research progress of SERS sensors based on hydrogen peroxide and related substances. *Crit. Rev. Anal. Chem.* **2023**, *54*, 3570–3591. [CrossRef] [PubMed]
11. Teodoro, K.B.; Migliorini, F.L.; Christinelli, W.A.; Correa, D.S. Detection of hydrogen peroxide (H_2O_2) using a colorimetric sensor based on cellulose nanowhiskers and silver nanoparticles. *Carbohydr. Polym.* **2019**, *212*, 235–241. [CrossRef]
12. Liu, J.; Li, M.; Liu, W.; Hao, Z.; Zhang, F.; Pang, H.; Zhang, R.; Zhang, L. Advances in non-enzymatic electrochemical materials for H_2O_2 sensing. *J. Electroanal. Chem.* **2024**, *954*, 118060. [CrossRef]
13. Huang, Y.; Wang, L.; Chen, B.; Zhang, Q.; Zhu, R. Detecting hydrogen peroxide reliably in water via ion chromatography: A method evaluation update and comparison in the presence of interfering components. *Environ. Sci. Water Res. Technol.* **2020**, *6*, 2396–2404. [CrossRef]
14. Chen, L.; Wei, L.; Ru, Y.; Weng, M.; Wang, L.; Dai, Q. A mini-review of the electro-peroxone technology for wastewaters: Characteristics, mechanism and prospect. *Chin. Chem. Lett.* **2023**, *34*, 108162. [CrossRef]
15. Schnabel, T.; Mehling, S.; Londong, J.; Springer, C. Hydrogen peroxide-assisted photocatalytic water treatment for the removal of anthropogenic trace substances from the effluent of wastewater treatment plants. *Water Sci. Technol.* **2020**, *82*, 2019–2028. [CrossRef]
16. Siddique, I. Unveiling the power of high-performance liquid chromatography: Techniques, applications, and innovations. *Eur. J. Adv. Eng. Technol.* **2021**, *8*, 79–84. [CrossRef]
17. Jawad, A.; Chen, Z.; Yin, G. Bicarbonate activation of hydrogen peroxide: A new emerging technology for wastewater treatment. *Chin. J. Catal.* **2016**, *37*, 810–825. [CrossRef]
18. Ahmad, T.; Iqbal, A.; Halim, S.A.; Uddin, J.; Khan, A.; El Deeb, S.; Al-Harrasi, A. Recent advances in electrochemical sensing of hydrogen peroxide (H_2O_2) released from cancer cells. *Nanomaterials* **2022**, *12*, 1475. [CrossRef]
19. Song, Y.; Wang, C.; Sha, J.; Liu, X.; Han, L.; Li, L. Photoelectrochemical sensor based on the sensitive interface of photosensitive electrode for the detection of hydrogen peroxide in dried bean curds. *J. Food Compos. Anal.* **2023**, *119*, 105237. [CrossRef]
20. Shamkhalichenar, H.; Choi, J.W. Non-enzymatic hydrogen peroxide electrochemical sensors based on reduced graphene oxide. *J. Electrochem. Soc.* **2020**, *167*, 037531. [CrossRef]
21. Saranchina, N.V.; Bazhenova, O.A.; Bragina, S.K.; Gavrilenko, N.A.; Volgina, T.N.; Gavrilenko, M.A. Stabilization of silver nanoparticles in a transparent polymethacrylate matrix while maintaining the capabilities of a colorimetric hydrogen peroxide sensor. *Chem. Pap.* **2024**, *78*, 8219–8224. [CrossRef]
22. Tang, J.; Li, F.; Liu, C.; Shu, J.; Yue, J.; Xu, B.; Liu, X.; Zhang, K.; Jiang, W. Attractive benzothiazole-based fluorescence probe for the highly efficient detection of hydrogen peroxide. *Anal. Chim. Acta* **2022**, *1214*, 339939. [CrossRef] [PubMed]
23. Shen, C.L.; Zheng, G.S.; Wu, M.Y.; Wei, J.Y.; Lou, Q.; Ye, Y.L.; Shan, C.X. Chemiluminescent carbon nanodots as sensors for hydrogen peroxide and glucose. *Nanophotonics* **2020**, *9*, 3597–3604. [CrossRef]
24. Shen, H.; Liu, H.; Wang, X. Surface construction of catalase-immobilized Au/PEDOT nanocomposite on phase-change microcapsules for enhancing electrochemical biosensing detection of hydrogen peroxide. *Appl. Surf. Sci.* **2023**, *612*, 155816. [CrossRef]
25. Clausmeyer, J.; Actis, P.; Córdoba, A.L.; Korchev, Y.; Schuhmann, W. Nanosensors for the detection of hydrogen peroxide. *Electrochem. Commun.* **2014**, *40*, 28–30. [CrossRef]

26. Liu, X.; Zhao, Z.; Shen, T.; Qin, Y. Graphene/Gold nanoparticle composite-based paper sensor for electrochemical detection of hydrogen peroxide. *Fuller. Nanotubes Carbon Nanostruct.* **2019**, *27*, 23–27. [CrossRef]
27. Gu, S.; Hsieh, C.T.; Mallick, B.C.; Fu, C.C.; Juang, R.S.; Gandomif, Y.A.; Kihm, K.D. Novel electrochemical sensor based on highly amidized graphene quantum dots to electrochemically detect hydrogen peroxide. *Appl. Surf. Sci.* **2020**, *528*, 146936. [CrossRef]
28. Feizabadi, M.; Soleymanpour, A.; Faridnouri, H.; Ajloo, D. Improving stability of biosensor based on covalent immobilization of horseradish peroxidase by γ-aminobutyric acid and application in detection of H_2O_2. *Int. J. Biol. Macromol.* **2019**, *136*, 597–606. [CrossRef]
29. Wei, Y.; Liu, Y.; He, Y.; Wang, Y. Mitochondria and lysosome-targetable fluorescent probes for hydrogen peroxide. *J. Mater. Chem. B* **2021**, *9*, 908–920. [CrossRef] [PubMed]
30. Alruwais, R.S.; Adeosun, W.A. Electrochemical detection of hydrogen peroxide using copper-based metal–organic frameworks: Nanoarchitectonics and sensing performance. *J. Inorg. Organomet. Polym. Mater.* **2024**, *34*, 14–37. [CrossRef]
31. Peng, M.; Zhao, Y.; Chen, D.; Tan, Y. Free-standing 3D electrodes for electrochemical detection of hydrogen peroxide. *ChemCatChem* **2019**, *11*, 4222–4237. [CrossRef]
32. da Silva Neves, M.M.P.; González-García, M.B.; Hernández-Santos, D.; Fanjul-Bolado, P. Future trends in the market for electrochemical biosensing. *Curr. Opin. Electrochem.* **2018**, *10*, 107–111. [CrossRef]
33. Baye, A.F.; Nguyen, H.T.; Kim, H. FeO/Fe_3C-assisted Fe_3O_4 redox sites as robust peroxidase mimics for colorimetric detection of H_2O_2. *Sens. Actuators B-Chem.* **2023**, *377*, 133097. [CrossRef]
34. Xu, L.; Zhang, Y.; Zhao, L.; Han, H.; Zhang, S.; Huang, Y.; Wang, Y.; Song, D.; Ma, P.; Ren, P.; et al. A neoteric dual-signal colorimetric fluorescent probe for detecting endogenous/exogenous hydrogen peroxide in cells and monitoring drug-induced hepatotoxicity. *Talanta* **2021**, *233*, 122578. [CrossRef]
35. Wu, Y.; Zhou, J.M.; Jiang, Y.S.; Wen, L.; He, M.J.; Xiao, Y.; Chen, J.Y. Silver nanoparticles@ metal-organic framework as peroxidase mimics for colorimetric determination of hydrogen peroxide and blood glucose. *Chin. J. Anal. Chem.* **2022**, *50*, 100187. [CrossRef]
36. Parveen, S.; Islam, S.N.; Ahmad, A. Mycological synthesis of ruthenium oxide quantum dots and their application in the colorimetric detection of H_2O_2. *Adv. Powder. Technol.* **2022**, *33*, 103861. [CrossRef]
37. Zhang, M.; Zhang, Y.; Yang, C.; Ma, C.; Tang, J. A novel smartphone-based colorimetric biosensor for reliable quantification of hydrogen peroxide by enzyme-inorganic hybrid nanoflowers. *Biochem. Eng. J.* **2021**, *167*, 107925. [CrossRef]
38. Peng, L.J.; Zhang, C.Y.; Zhang, W.Y.; Zhou, H.Y.; Yang, F.Q. The peroxidase-like catalytic activity of in situ prepared cobalt carbonate and its applications in colorimetric detection of hydrogen peroxide, glucose and ascorbic acid. *Colloids Surf. A* **2022**, *651*, 129744. [CrossRef]
39. Wu, L.; Zhou, X.; Wan, G.; Shi, S.; Wang, G. $NiFe_2O_4$/CNTs fabricated by atomic layer deposition as highly stable peroxidase mimics for sensitive colorimetric detection of hydrogen peroxide and glucose. *Mater. Res. Bull.* **2022**, *147*, 111637. [CrossRef]
40. Wang, J.; Zhou, Y.; Zeng, M.; Zhao, Y.; Zuo, X.; Meng, F.; Lu, Y. Zr (IV)-based metal-organic framework nanocomposites with enhanced peroxidase-like activity as a colorimetric sensing platform for sensitive detection of hydrogen peroxide and phenol. *Environ. Res.* **2022**, *203*, 111818. [CrossRef]
41. Zhang, H.; Ren, Q.; Lu, J.; Xu, Y.; Wang, Y.; Liu, S.; Luo, X. Simultaneous generation and immobilization of silver nanoparticles on cellulose membranes by hydrogen bond-assisted in-situ reaction for colorimetric detection of mercury ions and hydrogen peroxide. *Chem. Eng. J.* **2023**, *478*, 147264. [CrossRef]
42. Yu, K.; Li, M.; Chai, H.; Liu, Q.; Hai, X.; Tian, M.; Qu, L.; Xu, T.; Zhang, G.; Zhang, X. MOF-818 nanozyme-based colorimetric and electrochemical dual-mode smartphone sensing platform for in situ detection of H_2O_2 and H_2S released from living cells. *Chem. Eng. J.* **2023**, *451*, 138321. [CrossRef]
43. Zhang, W.Y.; Zhang, H.; Yang, F.Q. An economical and portable paper-based colorimetric sensor for the determination of hydrogen peroxide-related biomarkers. *Chemosensors* **2022**, *10*, 335. [CrossRef]
44. Xu, M.; Bunes, B.R.; Zang, L. Paper-based vapor detection of hydrogen peroxide: Colorimetric sensing with tunable interface. *ACS Appl. Mater. Interfaces* **2011**, *3*, 642–647. [CrossRef] [PubMed]
45. Kumar, K.S.; Ramakrishnappa, T. Green synthesized uncapped Ag colloidal nanoparticles for selective colorimetric sensing of divalent Hg and H_2O_2. *J. Environ.* **2021**, *9*, 105365. [CrossRef]
46. Ghohestani, E.; Tashkhourian, J.; Hemmateenejad, B. Colorimetric determination of peroxide value in vegetable oils using a paper based analytical device. *Food Chem.* **2023**, *403*, 134345. [CrossRef] [PubMed]
47. Wu, Y.; Lin, T.; Huang, J.; Chen, Y.; Zhong, J.; Guo, L.; Fu, F. Boron-and phenyl-doped graphitic carbon nitride (g-C_3N_4) nanosheets for colorimetric detection of hydrogen peroxide in soaked foods. *J. Nanosci. Nanotechnol.* **2019**, *19*, 4220–4227. [CrossRef]
48. Mu, Z.; Guo, J.; Li, M.; Wu, S.; Zhang, X.; Wang, Y. A sensitive fluorescence detection strategy for H_2O_2 and glucose by using aminated Fe–Ni bimetallic MOF as fluorescent nanozyme. *Microchim. Acta* **2023**, *190*, 81. [CrossRef] [PubMed]
49. An, J.; Park, S.; Jain, N.; Kim, Y.; Nimse, S.B.; Churchill, D.G. Novel mycophenolic acid precursor-based fluorescent probe for intracellular H_2O_2 detection in living cells and daphnia magna and zebrafish model systems. *Analyst* **2024**, *149*, 4477–4486. [CrossRef] [PubMed]

50. Fagadar-Cosma, E.; Plesu, N.; Lascu, A.; Anghel, D.; Cazacu, M.; Ianasi, C.; Fagadar-Cosma, G.; Fratilescu, I.; Epuran, C. Novel platinum-porphyrin as sensing compound for efficient fluorescent and electrochemical detection of H_2O_2. *Chemosensors* **2020**, *8*, 29. [CrossRef]
51. González-Ruiz, V.; Rajesh, J.; Olives, A.I.; Rocchi, D.; Gómez-Carpintero, J.; González, J.F.; Sridharan, V.; Martín, M.A.; Menéndez, J.C. Antioxidants as molecular probes: Structurally novel dihydro-m-terphenyls as turn-on fluorescence chemodosimeters for biologically relevant oxidants. *Antioxidants* **2020**, *9*, 605.
52. Olenin, A.Y. Methods of nonenzymatic determination of hydrogen peroxide and related reactive oxygen species. *J. Anal. Chem.* **2017**, *72*, 243–255. [CrossRef]
53. Li, M.; Lei, P.; Song, S.; Shuang, S.; Dong, C. Alizarin-based molecular probes for the detection of hydrogen peroxide and peroxynitrite. *Analyst* **2021**, *146*, 509–514. [CrossRef]
54. Yu, X.; Gong, Y.; Xiong, W.; Li, M.; Zhao, J.; Che, Y. Turn-on fluorescent detection of hydrogen peroxide and triacetone triperoxide via enhancing interfacial interactions of a blended system. *Anal. Chem.* **2019**, *91*, 6967–6970. [CrossRef]
55. Teniou, A.; Madi, I.A.; Mouhoub, R.; Marty, J.L.; Rhouati, A. One-step chemiluminescent assay for hydrogen peroxide analysis in water. *Chemosensors* **2023**, *11*, 455. [CrossRef]
56. Lee, S.H.; Kim, K.H.; Seo, S.E.; il Kim, M.; Park, S.J.; Kwon, O.S. Cytochrome C-decorated graphene field-effect transistor for highly sensitive hydrogen peroxide detection. *J. Ind. Eng. Chem.* **2020**, *83*, 29–34. [CrossRef]
57. Stoikov, D.; Shafigullina, I.; Shurpik, D.; Stoikov, I.; Evtugyn, G. A flow-through biosensor system based on pillar [3] arene [2] quinone and ferrocene for determination of hydrogen peroxide and uric acid. *Chemosensors* **2024**, *12*, 98. [CrossRef]
58. Xu, W.; Fei, J.; Yang, W.; Zheng, Y.; Dai, Y.; Sakran, M.; Zhang, J.; Zhu, W.; Hong, J.; Zhou, X. A colorimetric/electrochemical dual-mode sensor based on Fe_3O_4@MoS_2-Au NPs for high-sensitivity detection of hydrogen peroxide. *Microchem. J.* **2022**, *181*, 107825. [CrossRef]
59. Guo, X.; Cao, Q.; Liu, Y.; He, T.; Liu, J.; Huang, S.; Tang, H.; Ma, M. Organic electrochemical transistor for in situ detection of H_2O_2 released from adherent cells and its application in evaluating the in vitro cytotoxicity of nanomaterial. *Anal. Chem.* **2019**, *92*, 908–915. [CrossRef] [PubMed]
60. Zheng, C.; Wu, D.; Wang, T.; Xiao, J.; Yu, L. A label-free colorimetric assay based on gold nanoparticles for the detection of H_2O_2 and glucose. *Chemosensors* **2022**, *10*, 100. [CrossRef]
61. Zakaria, A.B.M.; Leszczynska, D. Electrochemically prepared unzipped single walled carbon nanotubes-MnO_2 nanostructure composites for hydrogen peroxide and glucose sensing. *Chemosensors* **2019**, *7*, 1. [CrossRef]
62. Shringi, A.K.; Kumar, R.; Dennis, N.F.; Yan, F. Two-dimensional tellurium nanosheets for the efficient nonenzymatic electrochemical detection of H_2O_2. *Chemosensors* **2024**, *12*, 17. [CrossRef]
63. Spanu, D.; Dhahri, A.; Binda, G.; Monticelli, D.; Pinna, M.; Recchia, S. Ultrafast electrochemical self-doping of anodic titanium dioxide nanotubes for enhanced electroanalytical and photocatalytic performance. *Chemosensors* **2023**, *11*, 560. [CrossRef]
64. Wiedemair, J.; van Dorp, H.D.; Olthuis, W.; van den Berg, A. Developing an amperometric hydrogen peroxide sensor for an exhaled breath analysis system. *Electrophoresis* **2012**, *33*, 3181–3186. [CrossRef] [PubMed]
65. Purwidyantri, A.; Tian, Y.C.; Saputra, G.M.A.; Prabowo, B.A.; Liu, H.L.; Yang, C.M.; Lai, C.S. Gold nanoframe array electrode for straightforward detection of hydrogen peroxide. *Chemosensors* **2021**, *9*, 37. [CrossRef]
66. Mihailova, I.; Krasovska, M.; Sledevskis, E.; Gerbreders, V.; Mizers, V.; Ogurcovs, A. Assessment of oxidative stress by detection of H_2O_2 in Rye samples using a CuO-and Co_3O_4-nanostructure-based electrochemical sensor. *Chemosensors* **2023**, *11*, 532. [CrossRef]
67. Han, J.; Kim, J.; Kim, B.K.; Park, K. Hydrogel-based electrodeposition of copper nanoparticles for selective detection for hydrogen peroxide. *Chemosensors* **2023**, *11*, 384. [CrossRef]
68. Lee, S.; Lee, Y.J.; Kim, J.H.; Lee, G.J. Electrochemical detection of H_2O_2 released from prostate cancer cells using Pt nanoparticle-decorated Rgo-CNT nanocomposite-modified screen-printed carbon electrodes. *Chemosensors* **2020**, *8*, 63. [CrossRef]
69. Luo, Y.; Wu, S.; Xiang, X.; Shu, J.; Fei, J. Fabricating process-electrochemical property correlation of laser-scribed graphene and smartphone-based electrochemical platform for portable and sensitive biosensing. *Biosens. Bioelectron.* **2023**, *237*, 115525. [CrossRef]
70. Kader, M.A.; Azmi, N.S.; Kafi, A.K.M.; Hossain, M.S.; Masri, M.F.B.; Ramli, A.N.M.; Tan, C.S. Synthesis and characterization of a multiporous SnO_2 nanofibers-supported Au nanoparticles-based amperometric sensor for the nonenzymatic detection of H_2O_2. *Chemosensors* **2023**, *11*, 130. [CrossRef]
71. Gligor, D.; Maicaneanu, S.A.; Varodi, C. Low-cost carbon paste Cu (II)-exchanged zeolite amperometric sensor for hydrogen peroxide detection. *Chemosensors* **2024**, *12*, 23. [CrossRef]
72. Zanoni, J.; Moura, J.P.; Santos, N.F.; Carvalho, A.F.; Fernandes, A.J.; Monteiro, T.; Rodrigues, J. Dual transduction of H_2O_2 detection using ZnO/laser-induced graphene composites. *Chemosensors* **2021**, *9*, 102. [CrossRef]
73. Xie, X.; Gao, N.; Zhu, L.; Hunter, M.; Chen, S.; Zang, L. PEDOT:PSS/PEDOT film chemiresistive sensors for hydrogen peroxide vapor detection under ambient conditions. *Chemosensors* **2023**, *11*, 124. [CrossRef]

74. Xie, X.; Gao, N.; Hunter, M.; Zhu, L.; Yang, X.; Chen, S.; Zang, L. PEDOT films doped with titanyl oxalate as chemiresistive and colorimetric dual-mode sensors for the detection of hydrogen peroxide vapor. *Sensors* **2023**, *23*, 3120. [CrossRef] [PubMed]
75. Karamoschos, N.; Tasis, D. Photocatalytic evolution of hydrogen peroxide: A minireview. *Energies* **2022**, *15*, 6202. [CrossRef]
76. Kim, G.; Lee, Y.E.K.; Kopelman, R. Hydrogen peroxide (H_2O_2) detection with nanoprobes for biological applications: A mini-review. In *Oxidative Stress Nanotechnology: Methods and Protocols*; Humana Press: Totowa, NJ, USA, 2013; pp. 101–114.
77. Żamojć, K.; Zdrowowicz, M.; Jacewicz, D.; Wyrzykowski, D.; Chmurzyński, L. Fluorescent probes used for detection of hydrogen peroxide under biological conditions. *Crit. Rev. Anal. Chem.* **2016**, *46*, 171–200. [CrossRef] [PubMed]
78. Hong, D.H.; Shim, H.S.; Ha, J.; Moon, H.R. MOF-on-MOF architectures: Applications in separation, catalysis, and sensing. *Bull. Korean Chem. Soc.* **2021**, *42*, 956–969. [CrossRef]
79. Schäferling, M.; Grögel, D.B.; Schreml, S. Luminescent probes for detection and imaging of hydrogen peroxide. *Microchim. Acta* **2011**, *174*, 1–18. [CrossRef]
80. Zheng, D.J.; Yang, Y.S.; Zhu, H.L. Recent progress in the development of small-molecule fluorescent probes for the detection of hydrogen peroxide. *TrAC Trend. Anal. Chem.* **2019**, *118*, 625–651. [CrossRef]
81. Rezende, F.; Brandes, R.P.; Schröder, K. Detection of hydrogen peroxide with fluorescent dyes. *Antioxid. Redox Signal.* **2018**, *29*, 585–602. [CrossRef]
82. Qiu, X.; Xin, C.; Qin, W.; Li, Z.; Zhang, D.; Zhang, G.; Huang, W. A novel pyrimidine based deep-red fluorogenic probe for detecting hydrogen peroxide in Parkinson's disease models. *Talanta* **2019**, *199*, 628–633. [CrossRef] [PubMed]
83. Zhang, X.; Xiao, W.; Xie, S.; Fan, G.; Shi, X.; Meng, H.; Yang, H. Low-density pt nanoarray-based hydrogen peroxide sensing platform and its application in trace sarcosine detection. *Electrochim. Acta* **2023**, *443*, 141952. [CrossRef]
84. Baranwal, J.; Barse, B.; Gatto, G.; Broncova, G.; Kumar, A. Electrochemical sensors and their applications: A review. *Chemosensors* **2022**, *10*, 363. [CrossRef]
85. Xiao, Q.; Xu, C. Research progress on chemiluminescence immunoassay combined with novel technologies. *TrAC Trend. Anal. Chem.* **2020**, *124*, 115780. [CrossRef]
86. Hey, Y.Y.; Bak, Y.; Seung, B.P.; Subba, R.C.; Kyung, H.S.; Kim, S.; Lee, J. Dual-modal iridium-based self-immolative chemosensors for differential responses against reactive oxygen species and their applications to detect diabetes. *Adv. Mater. Interfaces* **2023**, *10*, 2202408.
87. Riaz, M.A.; Chen, Y. Electrodes and electrocatalysts for electrochemical hydrogen peroxide sensors: A review of design strategies. *Nanoscale Horiz.* **2022**, *7*, 463–479. [CrossRef] [PubMed]
88. Chen, W.; Cai, S.; Ren, Q.Q.; Wen, W.; Zhao, Y.D. Recent advances in electrochemical sensing for hydrogen peroxide: A review. *Analyst* **2012**, *137*, 49–58. [CrossRef] [PubMed]
89. Chen, S.; Yuan, R.; Chai, Y.; Hu, F. Electrochemical sensing of hydrogen peroxide using metal nanoparticles: A review. *Microchim. Acta* **2013**, *180*, 15–32. [CrossRef]
90. Prakash, P.A.; Yogeswaran, U.; Chen, S.M. A review on direct electrochemistry of catalase for electrochemical sensors. *Sensors* **2009**, *9*, 1821–1844. [CrossRef] [PubMed]
91. Caval, M.; Sanna, C.; Marceddu, S.; Rocchitta, G.; Serra, P.A. The platinization of graphite composites turns widespread and low-cost materials into hydrogen peroxide sensors and high-value biosensor transducers. *Chemosensors* **2023**, *11*, 153. [CrossRef]
92. Mohan, S.; Dinesha, P.; Kumar, S. NO_x reduction behaviour in copper zeolite catalysts for ammonia SCR systems: A review. *Chem. Eng. J.* **2020**, *384*, 123253. [CrossRef]
93. Vijayaram, S.; Razafindralambo, H.; Sun, Y.Z.; Vasantharaj, S.; Ghafarifarsani, H.; Hoseinifar, S.H.; Raeeszadeh, M. Applications of green synthesized metal nanoparticles—A review. *Biol. Trace Elem. Res.* **2024**, *202*, 360–386. [CrossRef] [PubMed]
94. Zango, Z.U.; Khoo, K.S.; Garba, A.; Garba, Z.N.; Danmallam, U.N.; Aldaghri, O.; Ramesh, M.D. A review on titanium oxide nanoparticles modified metal-organic frameworks for effective CO_2 conversion and efficient wastewater remediation. *Environ. Res.* **2024**, *252*, 119024. [CrossRef]
95. Wang, W.; Liu, L.; Feng, J.; Yin, Y. Photocatalytic reversible color switching based on titania nanoparticles. *Small Methods* **2018**, *2*, 1700273. [CrossRef]
96. Li, X.; Shi, F.; Wang, L.; Zhang, S.; Yan, L.; Zhang, X.; Sun, W. Electrochemical biosensor based on horseradish peroxidase and black phosphorene quantum dot modified electrode. *Molecules* **2023**, *28*, 6151. [CrossRef] [PubMed]
97. Yang, F.; Ai, Y.; Li, X.; Wang, L.; Zhang, Z.; Ding, W.; Sun, W. Preparation of electrochemical horseradish peroxidase biosensor with black phosphorene–zinc oxide nanocomposite and their applications. *RSC Adv.* **2023**, *13*, 32028–32038. [CrossRef]
98. Zhao, L.; Li, C.; Qi, H.; Gao, Q.; Zhang, C. Electrochemical lectin-based biosensor array for detection and discrimination of carcinoembryonic antigen using dual amplification of gold nanoparticles and horseradish peroxidase. *Sens. Actuators B Chem.* **2016**, *235*, 575–582. [CrossRef]
99. Rahimi, P.; Joseph, Y. Enzyme-based biosensors for choline analysis: A review. *TrAC Trends Anal. Chem.* **2019**, *110*, 367–374. [CrossRef]

100. Sun, M.; Cui, C.; Chen, H.; Wang, D.; Zhang, W.; Guo, W. Enzymatic and non-enzymatic uric acid electrochemical biosensors: A Review. *ChemPlusChem* **2023**, *88*, e202300262. [CrossRef] [PubMed]
101. Shah, S.S.; Aziz, M.A.; Oyama, M.; Al-Betar, A.R.F. Controlled-potential-based electrochemical sulfide sensors: A review. *Chem. Rec.* **2021**, *21*, 204–238. [CrossRef] [PubMed]
102. Kajal, N.; Singh, V.; Gupta, R.; Gautam, S. Metal organic frameworks for electrochemical sensor applications: A review. *Environ. Res.* **2022**, *204*, 112320. [CrossRef] [PubMed]
103. Yang, H.; Xu, W.; Liang, X.; Yang, Y.; Zhou, Y. Carbon nanotubes in electrochemical, colorimetric, and fluorimetric immunosensors and immunoassays: A review. *Microchim. Acta* **2020**, *187*, 206. [CrossRef] [PubMed]
104. Han, D.; Vidic, J.; Jiang, D.; Loget, G.; Sojic, N. Photoinduced electrochemiluminescence immunoassays. *Anal. Chem.* **2024**, *96*, 18262–18268. [CrossRef]
105. Liu, H.; Weng, L.; Yang, C. A review on nanomaterial-based electrochemical sensors for H_2O_2, H_2S and NO inside cells or released by cells. *Microchim. Acta* **2017**, *184*, 1267–1283. [CrossRef]
106. Sohrabi, H.; Maleki, F.; Khaaki, P.; Kadhom, M.; Kudaibergenov, N.; Khataee, A. Electrochemical-based sensing platforms for detection of glucose and H_2O_2 by porous metal–organic frameworks: A review of status and prospects. *Biosensors* **2023**, *13*, 347. [CrossRef] [PubMed]
107. Li, J.; Hu, H.; Li, H.; Yao, C. Recent developments in electrochemical sensors based on nanomaterials for determining glucose and its byproduct H_2O_2. *J. Mater. Sci.* **2017**, *52*, 10455–10469. [CrossRef]
108. Zhang, R.; Chen, W. Recent advances in graphene-based nanomaterials for fabricating electrochemical hydrogen peroxide sensors. *Biosens. Bioelectron.* **2017**, *89*, 249–268. [CrossRef] [PubMed]
109. Gao, W.; Luo, X.; Liu, Y.; Zhao, Y.; Cui, Y. Development of an arduino-based integrated system for sensing of hydrogen peroxide. *Sens. Actuators Rep.* **2021**, *3*, 100045. [CrossRef]
110. Yang, X.; Qiu, W.; Gao, R.; Wang, Y.; Bai, Y.; Xu, Z.; Bao, S.J. MIL-47 (V) catalytic conversion of H_2O_2 for sensitive H_2O_2 detection and tumor cell inhibition. *Sens. Actuators B-Chem.* **2022**, *354*, 131201. [CrossRef]
111. Zhang, J.; Tan, Y.; Song, W.J. Zeolitic imidazolate frameworks for use in electrochemical and optical chemical sensing and biosensing: A review. *Microchim. Acta* **2020**, *187*, 234. [CrossRef] [PubMed]
112. Qu, C.; Liang, D.W. Novel electrochemical advanced oxidation processes with H_2O_2 generation cathode for water treatment: A review. *J. Environ.* **2022**, *10*, 107896. [CrossRef]
113. Oliveira, M.R.F.; Herrasti, P.; Furtado, R.F.; Melo, A.M.A.; Alves, C.R. Polymeric composite including magnetite nanoparticles for hydrogen peroxide detection. *Chemosensors* **2023**, *11*, 323. [CrossRef]
114. Mikołajczak, N.; Tańska, M.; Ogrodowska, D. Phenolic compounds in plant oils: A review of composition, analytical methods, and effect on oxidative stability. *Trends Food Sci. Technol.* **2021**, *113*, 110–138. [CrossRef]
115. Stepanov, E.V.; Shcherbakov, I.A. Physicochemical methods of studying hydrogen peroxide for biomedical applications. *Phys. Wave Phenom.* **2023**, *31*, 92–97. [CrossRef]
116. Kakeshpour, T.; Metaferia, B.; Zare, R.N.; Bax, A. Quantitative detection of hydrogen peroxide in rain, air, exhaled breath, and biological fluids by NMR spectroscopy. *Proc. Natl. Acad. Sci. USA* **2022**, *119*, e2121542119. [CrossRef]
117. Vahidpour, F.; Alghazali, Y.; Akca, S.; Hommes, G.; Schöning, M.J. An enzyme-based interdigitated electrode-type biosensor for detecting low concentrations of H_2O_2 vapor/aerosol. *Chemosensors* **2022**, *10*, 202. [CrossRef]
118. Michel, P.; Boudenne, J.L.; Robert-Peillard, F.; Coulomb, B. Analysis of homemade peroxide-based explosives in water: A review. *TrAC Trend. Anal. Chem.* **2023**, *158*, 116884. [CrossRef]
119. Romolo, F.S.; Connell, S.; Ferrari, C.; Suarez, G.; Sauvain, J.J.; Hopf, N.B. Locating bomb factories by detecting hydrogen peroxide. *Talanta* **2016**, *160*, 15–20. [CrossRef] [PubMed]
120. Yan, J.; Jiang, J.; He, L.; Chen, L. Mitochondrial superoxide/hydrogen peroxide: An emerging therapeutic target for metabolic diseases. *Free Radic. Biol. Med.* **2020**, *152*, 33–42. [CrossRef] [PubMed]
121. Wang, L.; Hou, X.; Fang, H.; Yang, X. Boronate-based fluorescent probes as a prominent tool for H_2O_2 sensing and recognition. *Curr. Med. Chem.* **2022**, *29*, 2476–2489. [CrossRef]
122. Li, J.; Xu, N.; Zhang, Y.; Dong, H.; Li, C. Research progress of heterogeneous photocatalyst for H_2O_2 production: A mini review. *Chin. Chem. Lett.* **2024**, 110470. [CrossRef]
123. Jarnda, K.V.; Wang, D.; Anaman, R.; Johnson, V.E.; Roberts, G.P.L.; Johnson, P.S.; Jallawide, B.W.; Kai, T.; Ding, P. Recent advances in electrochemical non-enzymatic glucose sensor for the detection of glucose in tears and saliva: A review. *Sens. Actuators A-Phys.* **2023**, *363*, 114778. [CrossRef]
124. Do, H.H.; Kim, S.Y.; Van Le, Q. Development of non-precious metal oxide-based electrodes for enzyme-free glucose detection: A review. *Microchem. J.* **2023**, *193*, 109202. [CrossRef]
125. Lee, W.C.; Kim, K.B.; Gurudatt, N.G.; Hussain, K.K.; Choi, C.S.; Park, D.S.; Shim, Y.B. Comparison of enzymatic and non-enzymatic glucose sensors based on hierarchical Au-Ni alloy with conductive polymer. *Biosens. Bioelectron.* **2019**, *130*, 48–54. [CrossRef] [PubMed]

126. He, C.; Asif, M.; Liu, Q.; Xiao, F.; Liu, H.; Xia, B.Y. Noble metal construction for electrochemical nonenzymatic glucose detection. *Adv. Mater. Technol.* **2023**, *8*, 2200272. [CrossRef]
127. Xue, M.; Mao, W.; Chen, J.; Zheng, F.; Chen, W.; Shen, W.; Tang, S. Application of Au or Ag nanomaterials for colorimetric detection of glucose. *Analyst* **2021**, *146*, 6726–6740. [CrossRef] [PubMed]
128. Okoye, C.N.; Chinnappareddy, N.; Stevens, D.; Kamunde, C. Factors affecting liver mitochondrial hydrogen peroxide emission. *Comp. Biochem. Phys. B* **2022**, *259*, 110713. [CrossRef] [PubMed]
129. Qureshi, M.K.; Gawroński, P.; Munir, S.; Jindal, S.; Kerchev, P. Hydrogen peroxide-induced stress acclimation in plants. *Cell. Mol. Life Sci.* **2022**, *79*, 129. [CrossRef]
130. Smirnoff, N.; Arnaud, D. Hydrogen peroxide metabolism and functions in plants. *New Phytol.* **2019**, *221*, 1197–1214. [CrossRef] [PubMed]